Zoological Journal of the Linnean Society, 2024, XX, 1–19
https://doi.org/10.1093/zoolinnean/zlae058
Advance access publication 30 May 2024
Original Article

OXFORD

Original Article

The pharynx of the iconic stem-group chondrichthyan *Acanthodes* Agassiz, 1833 revisited with micro-computed tomography

Richard P. Dearden[1,2,*], Anthony Herrel[3,4,5,6] and Alan Pradel[2]

[1]Naturalis Biodiversity Center, Darwinweg 2, 2333 CR, Leiden, The Netherlands
[2]CR2P, Centre de Recherche en Paléontologie–Paris, Muséum national d'Histoire naturelle, Sorbonne Université, Centre National de la Recherche Scientifique, 75005 Paris cedex 05, France
[3]UMR 7179 (MNHN-CNRS) MECADEV, Département Adaptations du Vivant, Muséum National d'Histoire Naturelle, 75005 Paris, France
[4]Department of Biology, Evolutionary Morphology of Vertebrates, Ghent University, K. L. Ledeganckstraat 35, 9000 Ghent, Belgium
[5]Department of Biology, University of Antwerp, Groenenborgerlaan 171, 2020 Antwerp, Belgium
[6]Naturhistorisches Museum Bern, Bernastrasse 15, 3005 Bern, Switzerland

[*]Corresponding author. Naturalis Biodiversity Center, Postbus 9517, 2300 RA Leiden, The Netherlands. E-mail: richard.dearden@naturalis.nl

ABSTRACT

Acanthodes has long been the primary source of information on the pharyngeal skeleton of 'acanthodians'. Because of this its anatomy has played a disproportionate role in attempts to understand the evolution of the jawed vertebrate pharynx and the clade as a whole. However, the anatomy of the pharynx of *Acanthodes*, now understood to be a stem-group chondrichthyan, remains poorly characterized and subject to several competing interpretations. We used computed tomography to image the articulated pharyngeal skeletons of three specimens of *Acanthodes confusus* from Lebach, Germany. *Acanthodes* has a *mélange* of osteichthyan-like and chondrichthyan-like morphologies in its pharyngeal skeleton. Like many other chondrichthyans, *Acanthodes* lacked hypohyals, and had four pairs of posteriorly oriented pharyngobranchials. Like osteichthyans, *Acanthodes* possessed an interhyal, but lacked the separate infra- and supra-pharyngobranchial elements present in osteichthyans and the crown-chondrichthyan *Ozarcus*. Using these new data we built and animated a digital 3D model of the pharyngeal endoskeleton in *Acanthodes*, showing that the jaws could have swung outwards during the opening cycle, increasing the anteriorly facing area of the gape for suspension feeding. These new data provide a more definitive picture of the anatomy of a taxon that has long been of great significance in early vertebrate palaeontology.

Keywords: acanthodian; branchial skeleton; chondrichthyan; computed tomography; Permian; pharynx

INTRODUCTION

The Late Palaeozoic stem-group chondrichthyan *Acanthodes* Agassiz, 1833 has been a focal point of efforts to understand the evolution of the vertebrate pharynx since the 19th century (Reis 1890, 1894, 1895, 1896, Dean 1907, Watson 1937, Miles 1968, 1973, Nelson 1968, Jarvik 1977, Heidtke 2011, 2015, Davis *et al.* 2012, Brazeau and de Winter 2015). The exceptional preservation of the delicate and easily disarticulated visceral skeleton in numerous fossils of *Acanthodes confusus* Heidtke, 2011 from the Early Permian of Lebach, Germany makes it one of very few Palaeozoic taxa, and for a long time the only 'acanthodian' stem-group chondrichthyan, which preserves information on the anatomy of the pharyngeal skeleton. Recently a number of three-dimensionally preserved pharyngeal skeletons of Palaeozoic chondrichthyans have been described in great detail using computed tomographic (CT) methods, including other stem-group chondrichthyans (Coates *et al.* 2018, Dearden *et al.* 2019, Maisey *et al.* 2019) as well as Palaeozoic crown-group members (Pradel *et al.* 2014, 2021, Coates *et al.* 2019, 2021, Frey *et al.* 2019, 2020, Hodnett *et al.* 2021, Dearden *et al.* 2023, Klug *et al.* 2023), which show a wide range of feeding modes. However, *Acanthodes* remains important as one of the best preserved of these and is further interesting from a functional perspective as a very late-occurring acanthodian, seemingly adapted to be a filter feeder, in the broader ecological context of the Late Palaeozoic (Stack *et al.* 2020).

Despite there being numerous, intensively-studied fossils in museum collections that preserve the pharyngeal skeleton of

Received 6 October 2023; revised 30 March 2024; accepted 16 April 2024

Acanthodes its anatomy remains uncertain. Interpretations of the pharynx of *Acanthodes* remain based almost entirely [but see (Dearden and Giles 2021)] on acid-prepared moulds, studied by making casts either physically (Miles 1973) or more recently digitally (Brazeau and de Winter 2015). While many detailed anatomical studies of *A. confusus* have been carried out using these, each cast shows only those elements on the split face of the concretion, making it challenging to understand the spatial relationship and shape of the numerous elements of the complex pharyngeal skeleton. This is further exacerbated by the unusually segmented ossification pattern of the visceral skeleton in *Acanthodes*. The resulting interpretational ambiguities have led to conflicting reconstructions of the pharyngeal anatomy of *Acanthodes* (Fig. 1), with very different interpretations of characters such as the hyoid arch components and orientation of pharyngeal elements (Reis 1896, Dean 1907, Watson 1937, Miles 1964, 1965, 1968, 1973, Nelson 1968, Jarvik 1977). Several of the variable features of these reconstructions are potentially important phylogenetic characters and recent reassessment of other aspects of the endoskeletal anatomy of *Acanthodes* have had influential phylogenetic implications (Davis *et al.* 2012, Brazeau and de Winter 2015). More generally they feed into hypotheses of the origins of gnathostome pharyngeal anatomy (Nelson 1968, Pradel *et al.* 2014, Coates *et al.* 2018, Dearden *et al.* 2019).

Here we aim to resolve uncertainty in the pharyngeal anatomy of *Acanthodes confusus* by carrying out a detailed redescription. Rather than using mouldic specimens, we do this by CT scanning concretions from Lebach which have not been acid prepared. Using the resulting 3D models we reconstruct the anatomy of the visceral skeleton of *Acanthodes confusus*, and reappraise this anatomy and its functional morphology in the context of what is now known about the pharyngeal anatomy of Palaeozoic gnathostomes.

MATERIAL AND METHODS

Institutional abbreviations

MNHN, Muséum national d'Histoire naturelle, Paris, France; NHMUK, Natural History Museum, London, United Kingdom.

Specimens

In this study we describe three specimens of *Acanthodes confusus* from the collections of the MNHN: MNHN-F-SAA21 (Fig. 2), MNHN-F-SAA20 (Fig. 3), and MNHN-F-SAA24 (Fig. 4). The majority of Lebach vertebrate remains were prepared using acid to create moulds, so that they could be studied using peels and casts (Miles 1973). We selected these three because they visibly preserve articulated visceral skeletons which have not been extensively acid prepared. At the time of writing, in the MNHN collections these specimens are assigned to *Acanthodes bronni* Agassiz, 1833; the well-ossified *Acanthodes* taxon from Lebach has now been revised and placed in the species *Acanthodes confusus* (Heidtke 2011, Coates *et al.* 2018) and we follow this taxonomic assignment here.

3D data acquisition

We scanned the specimens using micro-computed tomography (μCT) on a Baker Hughes Digital Solutions v|tome|x 240 L μCT scanner with a tungsten target and an exposure time of 1000 ms on the MNHN AST-RX platform. MNHN-F-SAA20 was scanned with a 1 mm Cu and a 0.5 Sn filter at 200 kV and 350 μA, resulting in a voxel size of 59 μm. MNHN-F-SAA21 was scanned with a 0.3 mm Cu filter at 185 kV and 350 μA, resulting in a voxel size of 64 μm. MNHN-F-SAA24 was scanned with a 1 mm Cu filter at 220 kV and 250 μA, resulting in a voxel size of 56 μm. We processed the tomographic data using Materialise Mimics 19.0, manually segmenting the data using the 'Edit Masks' and 'Multiple Slice Edit' tools. We then rendered the resulting three-dimensional (3D) models in the freeware Blender 3.30 (blender.org) to create images and videos.

Reconstruction and gape animation

With the aim of investigating the functional morphology of the mandibular skeleton we reconstructed the visceral skeleton of *Acanthodes* in Blender using models from the three specimens described here. What we judged to be the best-preserved example of each element from either side was used for the reconstruction, and then mirrored across the x-axis. The jaws, ceratohyal, and hyomandibula were taken from MNHN-F-SAA21, and the branchial arches, braincase elements, interhyal, and basibranchial from MNHN-F-SAA24. All elements were scaled using the relative sizes of the jaws in either specimen. In the case of the jaws and hyoid arch we tidied the surface models by mending holes and smoothing surfaces. Unmineralized sections of bones were interpolated using the Blender sculpting tool.

Models were then rearranged into an approximation of life position based on the relative articulation between the different jaw and braincase elements and with living gnathostomes as a reference (Dearden *et al.* 2021). First the braincase elements were placed centrally, using the reconstruction of Davis *et al.* (2012) and dorsoventrally flattened casts (e.g. NHMUK PV P 49995) as a guide. The palatoquadrates were then placed in contact with the braincase using the articulation points on the otic process and basal process (Miles 1973). Meckel's cartilages were placed in contact with the palatoquadrates using their articulation point, and the anterior tip was placed medially so as to be close to its antimere. The distal tips of the hyomandibulae were aligned with the braincase by approximating their articulation with the ventrolateral angle (Brazeau and de Winter 2015). The interhyals and the proximal tip of the ceratohyal were placed below the proximal tip of the hyomandibula by using their relative positions in MNHN-F-SAA24 and NHM PV P 49990. The basibranchial was placed medially at the level of the mandibles and its articulation points with the ceratohyal used to determine its position antero-posteriorly. The branchial arches were placed posterior to the hyoid arch using their arrangement in all specimens as a guide.

To investigate the jaw opening mechanism we animated the abduction of the jaws and hyoid arch in Blender. A cylindrical geometrical primitive was manually aligned with the articulations between the palatoquadrate and the braincase (Bishop *et al.* 2021), and its long axis used as the axis around which the palatoquadrates were abducted. The same procedure was carried out at the articulation between the Meckel's cartilage and palatoquadrate. Both of these ensured that each rotation happened with a single degree of freedom. The palatoquadrate was animated to abduct to 30° around the articulation with the

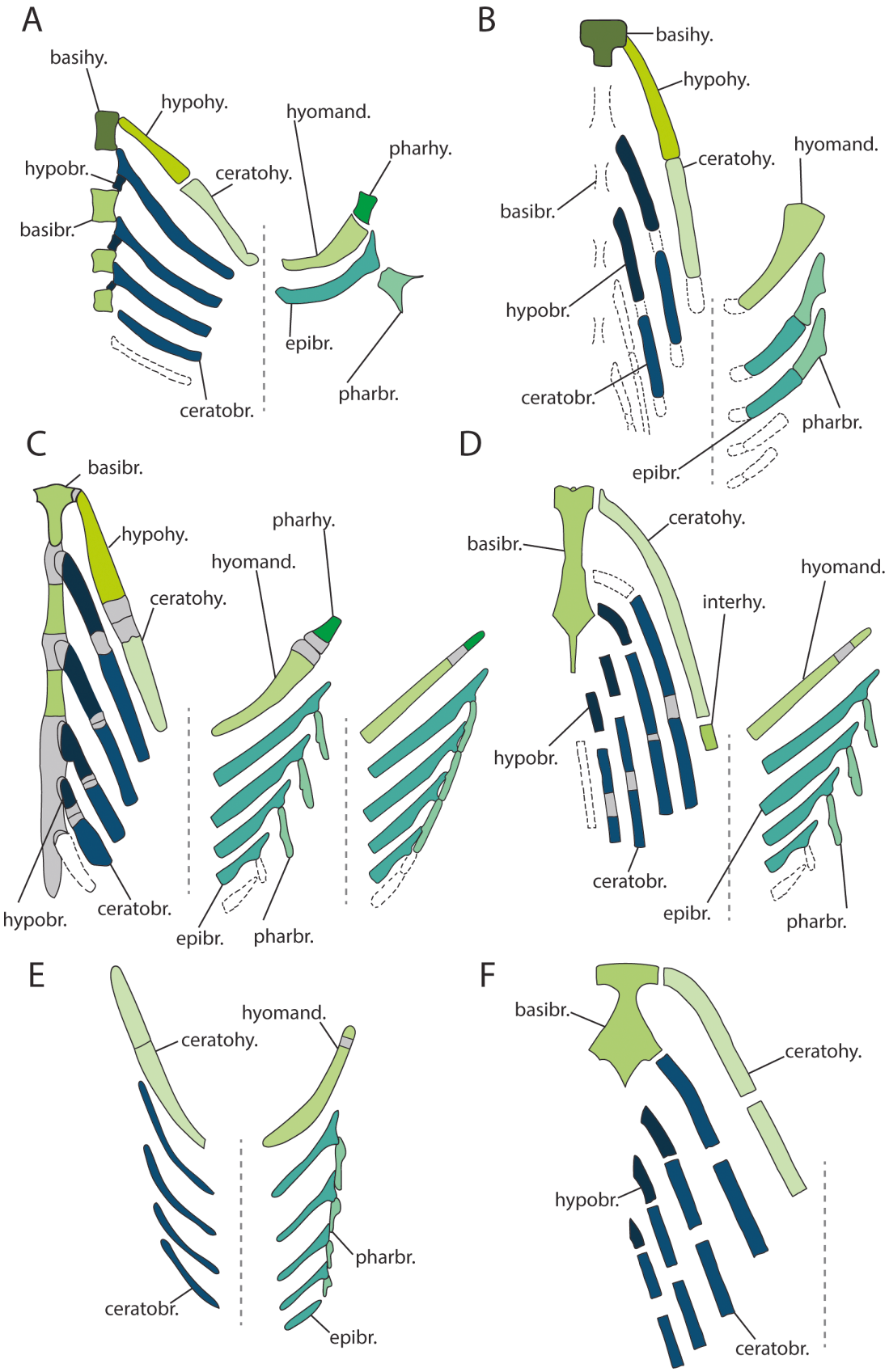

Figure 1. Previous reconstructions of the hyoid and branchial arch skeleton in *Acanthodes*. A, Reis (1896). B, Watson (1937). C, Nelson (1968) with both alternate reconstructions of pharyngobranchial orientation. D, Miles (1973). E, Jarvik (1977). F, Gardiner (1984). Terminology has been standardized to match terms used in this study. Abbreviations: basibr., basibranchial; basihy., basihyal; ceratobr., ceratobranchials; ceratohy., ceratohyal; epibr., epibranchial; hyomand., hyomandibula; hypohy., hypohyal; interhy., interhyal; pharbr., pharyngobranchials; pharhy., pharyngohyal. Matching colours denote serially homologous elements. Grey indicates inferred areas of cartilage. Black dashed lines indicate hypothetical elements. Vertical grey dashed line indicates junction of dorsal and ventral branchial skeleton. All reconstructions are shown as if spread horizontally, with anterior upwards.

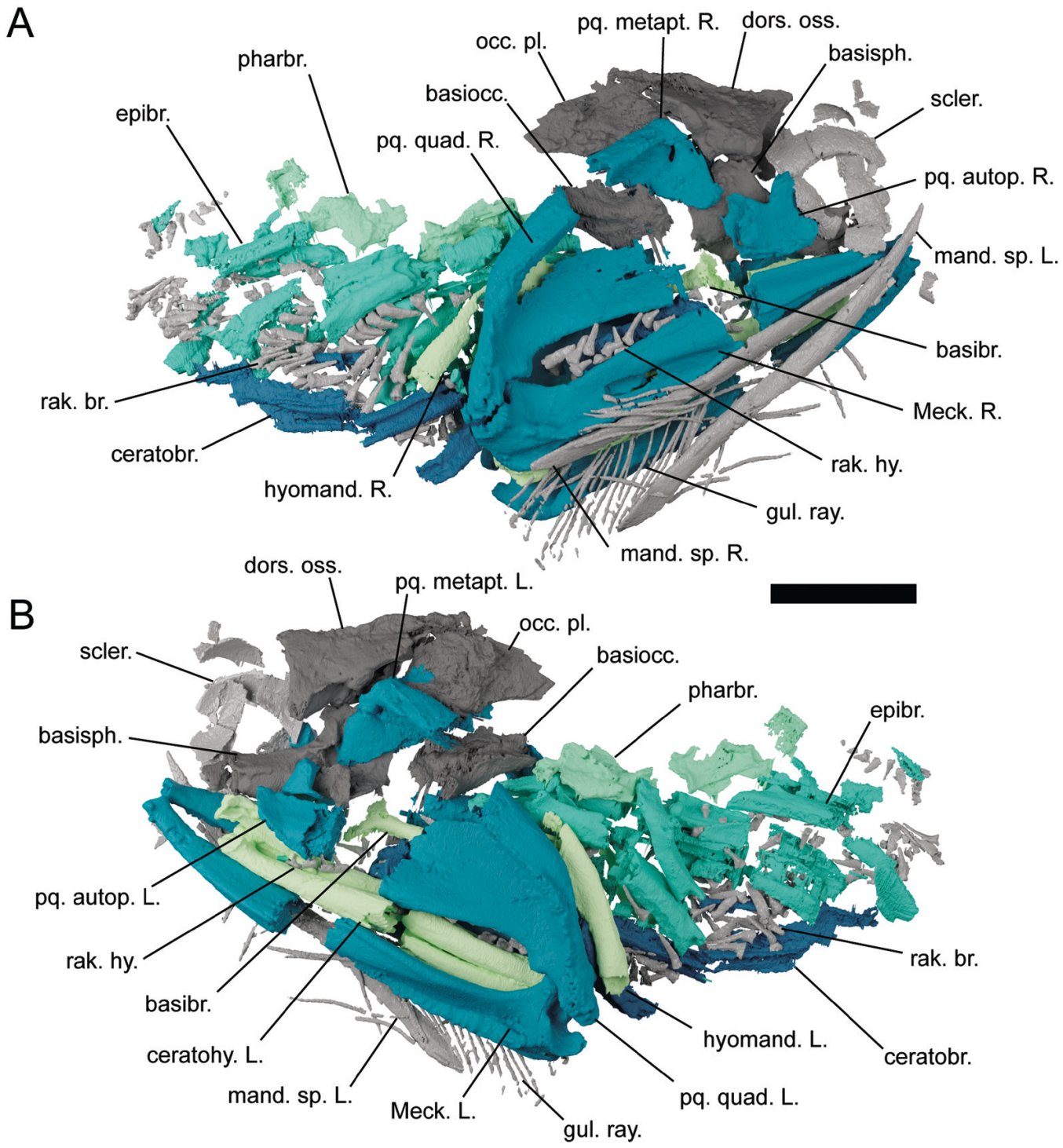

Figure 2. The head skeleton of *Acanthodes confusus* MNHN-F-SAA21, visualized using computed tomography. A, in right lateral view. B, in left lateral view. Abbreviations: basibr., basibranchial; basiocc., basioccipital; basisph., basisphenoid; ceratobr., ceratobranchials; ceratohy., ceratohyal; dors. oss., dorsal ossification of neurocranium; epibr., epibranchial; gul. ray., gular rays; hyomand., hyomandibula; L., left; mand. sp., mandibular splint; Meck., Meckel's cartilage; occ. pl., occipital plate; pharbr., pharyngobranchials; pq. autop., palatoquadrate autopalatine; pq. metapt., palatoquadrate metapterygoid; pq. quad., palatoquadrate quadrate; R., right; rak. br., branchial rakers; rak. hy., hyoid rakers; scler., sclerotic ring. Colour scheme: blue-greens, elements of visceral endoskeleton with mandibular arch, hyoid arch, hypobranchials, ceratobranchials, epibranchials, and pharyngobranchials coloured independently; dark grey, cranial and pectoral endoskeleton; light grey, elements of the dermal skeleton. Scale bar = 20 mm.

braincase. The Meckel's cartilage was animated to abduct to 20°. These angles were chosen on the basis that beyond them the tips of the mandibles started to move significantly apart. A cylinder was also placed at the distal tip of the hyomandibula, assuming its rotation was perpendicular to the axis of its broad end. The hyomandibula was animated to rotate around this

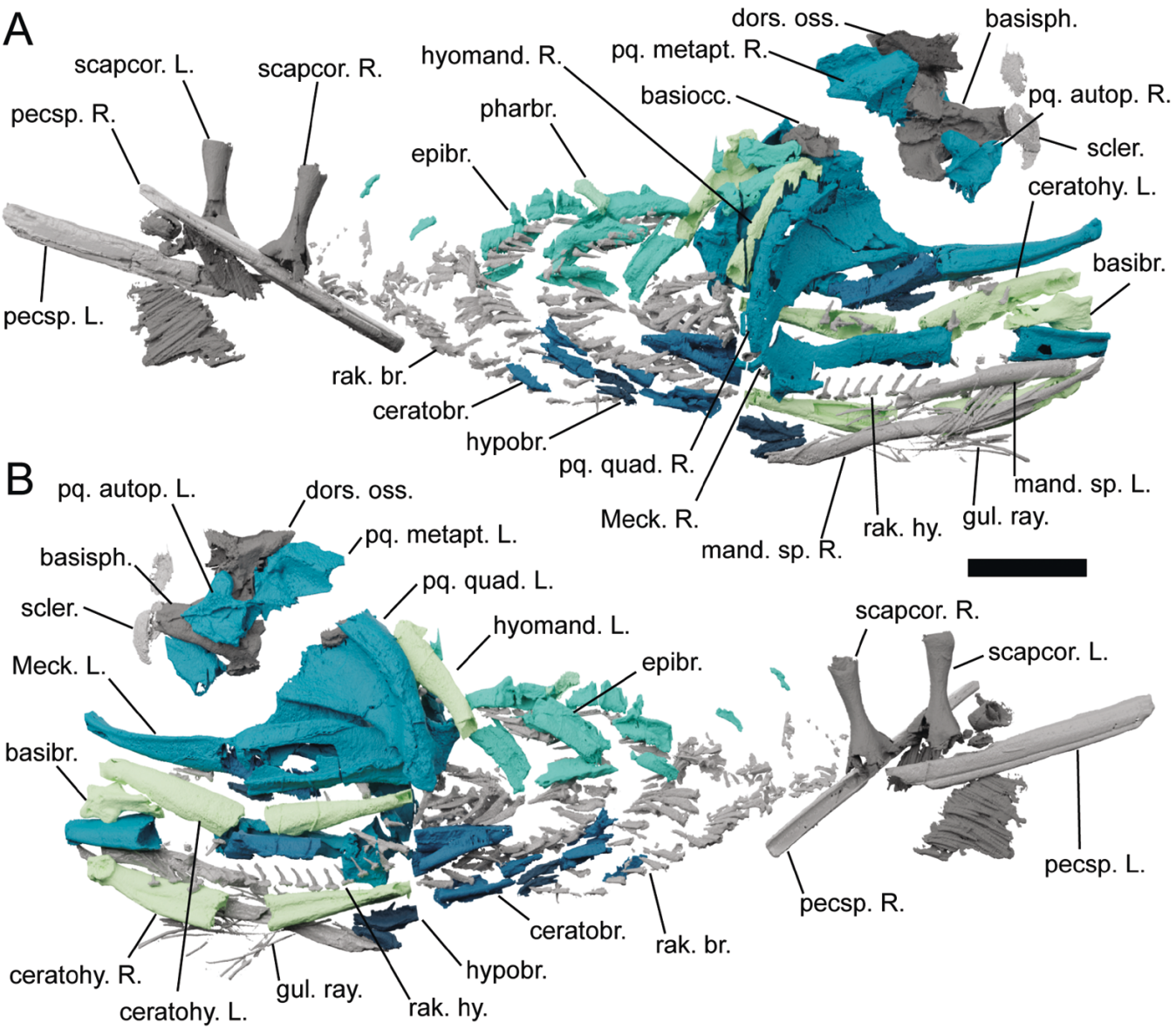

Figure 3. The head skeleton of *Acanthodes confusus* MNHN-F-SAA20, visualized using computed tomography. A, in right lateral view. B, in left lateral view. Abbreviations: basibr., basibranchial; basiocc., basioccipital; basisph., basisphenoid; ceratobr., ceratobranchials; ceratohy., ceratohyal; dors. oss., dorsal ossification of neurocranium; epibr., epibranchial; gul. ray., gular rays; hyomand., hyomandibula; hypobr., hypobranchials; L., left; mand. sp., mandibular splint; Meck., Meckel's cartilage; pharbr., pharyngobranchials; pecsp., pectoral fin spine; pq. autop., palatoquadrate autopalatine; pq. metapt., palatoquadrate metapterygoid; pq. quad., palatoquadrate quadrate; R., right; rak. br., branchial rakers; rak. hy., hyoid rakers; scapcor., scapulocoracoids; scler., sclerotic ring. Colour scheme: blue-greens, elements of visceral endoskeleton with mandibular arch, hyoid arch, hypobranchials, ceratobranchials, epibranchials, and pharyngobranchials coloured independently; dark grey, cranial and pectoral endoskeleton; light grey, elements of the dermal skeleton. Scale bar = 20 mm.

axis to and maintain its distance from the back of the mandible. The basibranchial was animated to move posteroventrally and an armature was then used to simulate the movement of the ceratohyals. An armature was also assigned to each branchial arch and used to simulate their movement for the reconstruction.

RESULTS

All three specimens have collapsed laterally, but the 3D shape of individual pharyngeal elements is retained and is consistent on either side of specimens. Between the three specimens most of the known endoskeleton of *Acanthodes* is preserved (Figs 2–4) including the jaws, hyoid arch, branchial skeleton, braincase, and shoulder girdle. Here we concentrate on the visceral skeleton: the braincase and shoulder girdle will be the focus of future descriptions. Generally speaking the details of the visceral skeleton of *Acanthodes* matches the detailed accounts of Miles (1964, 1965, 1968, 1973; Figs 5–10). In this account we generally follow Miles' terminology; a comparison of the terminology we use to that used by previous authors is given in Supporting Information, Table S1. A drawing of our pharyngeal reconstruction is given in Figure 11.

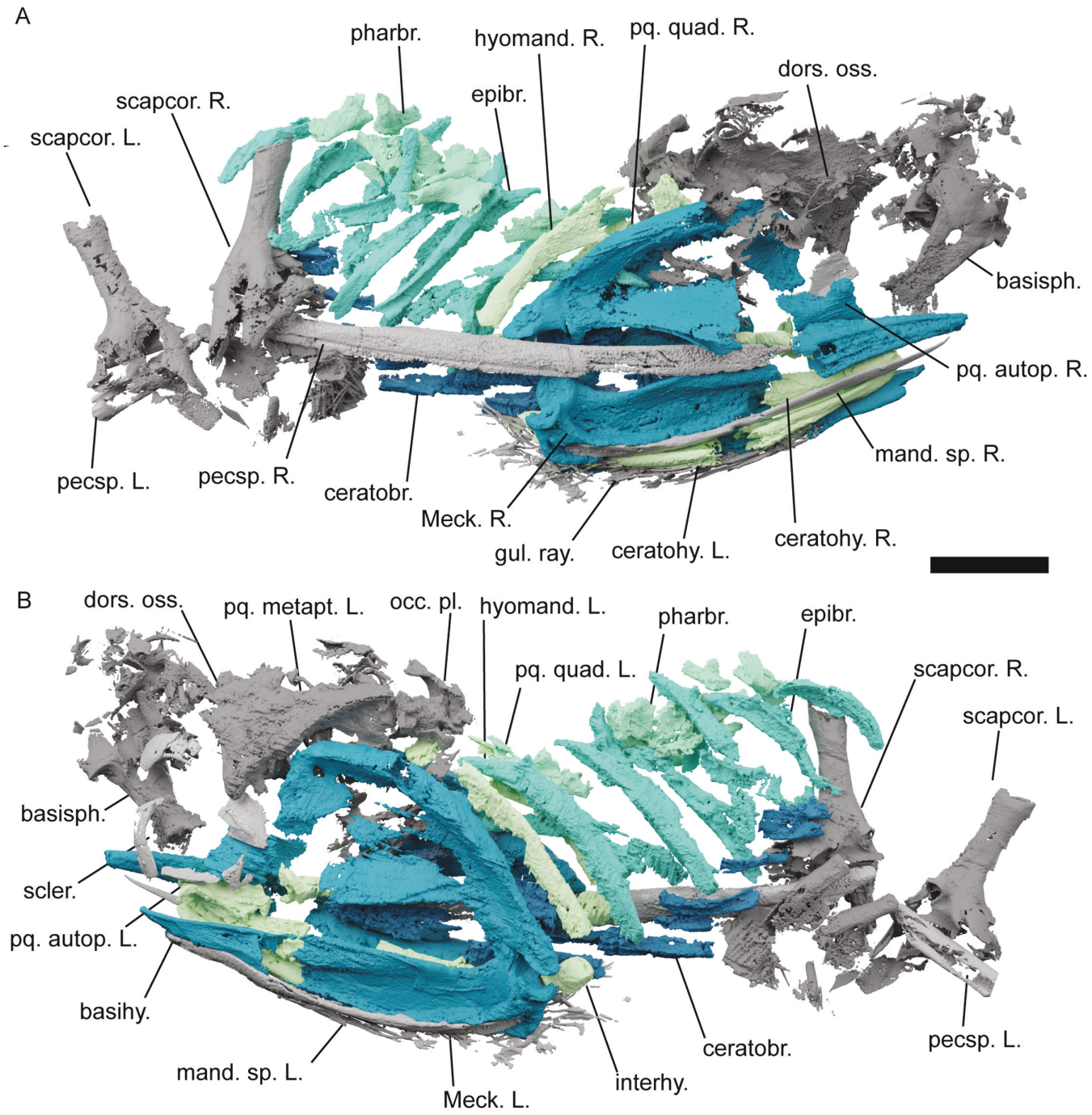

Figure 4. The head skeleton of *Acanthodes confusus* MNHN-F-SAA24, visualized using computed tomography. A, in right lateral view. B, in left lateral view. Abbreviations: basisph., basisphenoid; ceratobr., ceratobranchials; ceratohy., ceratohyal; dors. oss., dorsal ossification of neurocranium; epibr., epibranchial; gul. ray., gular rays; hyomand., hyomandibula; interhy., interhyal; L., left; mand. sp., mandibular splint; Meck., Meckel's cartilage; occ. pl., occipital plate; pharbr., pharyngobranchials; pecsp., pectoral fin spine; pq. autop., palatoquadrate autopalatine; pq. metapt., palatoquadrate metapterygoid; pq. quad., palatoquadrate quadrate; R., right; scapcor., scapulocoracoids; scler., sclerotic ring. Colour scheme: blue-greens, elements of visceral endoskeleton with mandibular arch, hyoid arch, hypobranchials, ceratobranchials, epibranchials, and pharyngobranchials coloured independently; dark grey, cranial and pectoral endoskeleton; light grey, elements of the dermal skeleton. Scale bar = 20 mm.

All endoskeletal elements in *A. confusus* comprise a heavily mineralized outer shell surrounding an internal space (Fig. 5) that was presumably filled with unmineralized cartilage in life. Our scan data is of insufficient high resolution to show the histology of the outer tissue, but Ørvig (1951) interpreted the same tissue as perichondral bone in thin sections of acanthodians including *Acanthodes* specimens from Lebach on the basis of the tissue having fusiform cell spaces with canaliculi and Sharpey's fibre attachments, albeit lacking lamination or vascular canals. This perichondral bony tissue is distinct from the

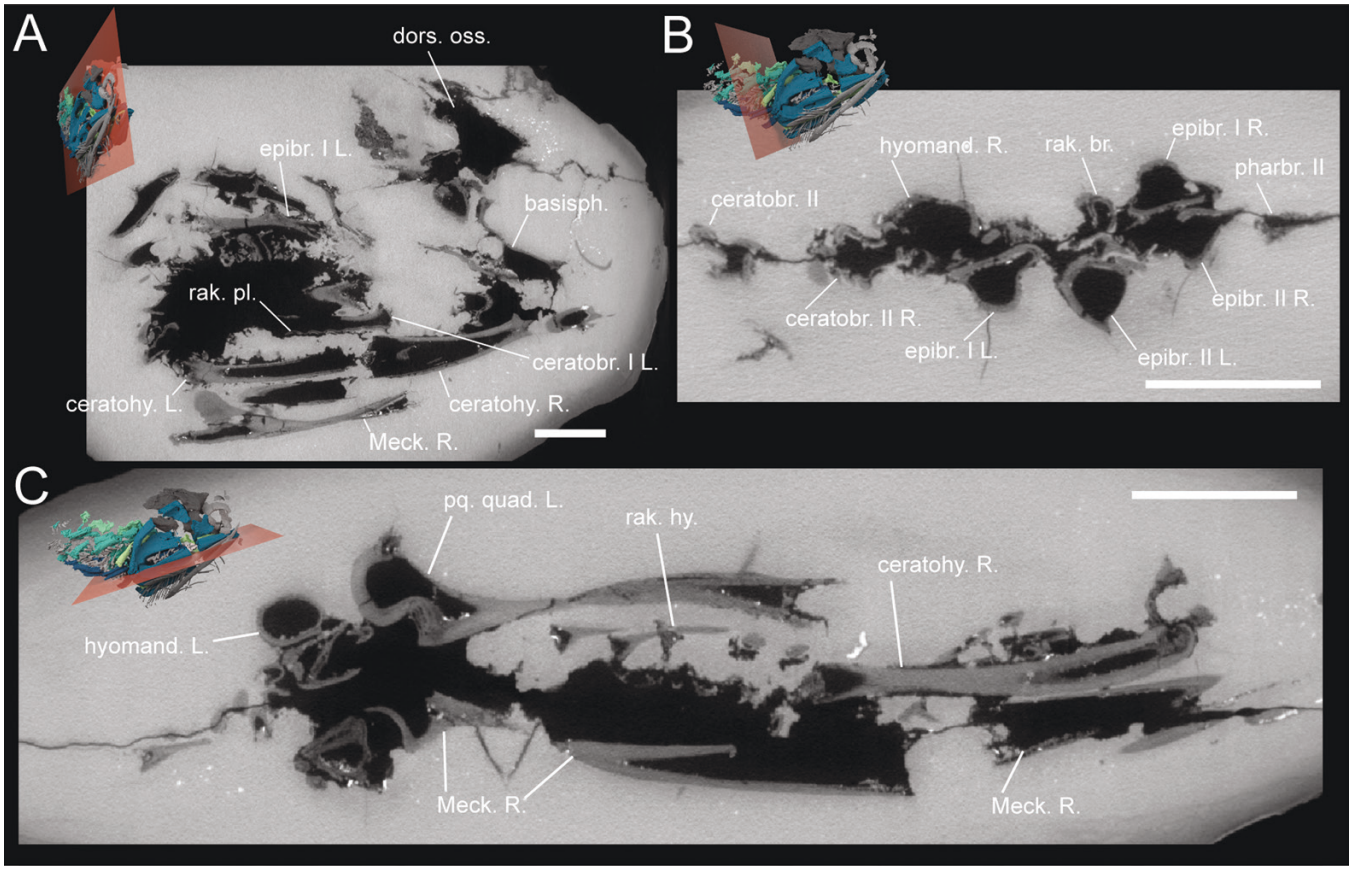

Figure 5. Sections through tomograms from the scan data for MNHN-F-SAA21. A, sagittal section. B, transverse section. C, coronal section. Abbreviations: basisph., basisphenoid; rak. br., branchial rakers; ceratobr., ceratobranchials; ceratohy., ceratohyal; dors. oss., dorsal ossification of neurocranium; epibr., epibranchial; hyomand., hyomandibula; rak. hy., hyoid rakers; L., left; Meck., Meckel's cartilage; pharbr., pharyngobranchials; R., right; rak. pl., plinth for branchial raker. Red plane indicates plane of bisection. Scale bar = 10 mm. In tomograms lighter values represent more radiodense materials: light grey areas are the matrix, dark grey areas are skeletal tissues, and black areas are air spaces.

varied cartilage tissues that have been described in other stem-chondrichthyans (Burrow *et al.* 2018, 2020, Maisey *et al.* 2020, Burrow and Blaauwen 2021). The thickness of this tissue is variable through the skeleton, for example being thicker in the mandibular arches than in the branchial arches, particularly around the mandibular articulation (Fig. 5C). This probably reflects the function of different elements analogously to varying thicknesses in the prismatic tesselate calcified cartilage in extant and extinct chondrichthyans (Maisey *et al.* 2020).

Mandibular arch

The mandibular arch (Fig. 6) comprises a palatoquadrate and Meckel's cartilage, the morphology of which largely confirm the description of Miles (1968, 1973). The three ossifications of the palatoquadrates are unfinished and have open margins where they would have been joined by uncalcified cartilage. When reconstructed they conform with Miles' account of their articulations with the neurocranium (Miles 1968). The anterior edge of the autopalatine is finished, with no evidence for an anteriorly extending palatine commissure (Jarvik 1977). Like the palatoquadrate ossifications, the two ossifications of the Meckel's cartilage are unfinished towards the centre of the element. The relationship between the Meckel's cartilage and the dermal mandibular splint matches the description of Dearden and Giles (2021). The cup-like anterior tip to the Meckel's cartilages suggests a well-developed but mobile connective-tissue attachment between them, and may be a character uniting a subset of stem-group chondrichthyans (Dearden and Giles 2021). The articulation between the palatoquadrate and Meckel's cartilage confirm the description of Miles (1973), although the preglenoid process is notably more rounded than in that reconstruction. There is no pronounced retroarticular flange as in *Gogoselachus* and *Tristychius* (Long *et al.* 2015, Coates *et al.* 2019, Frey *et al.* 2020). When closed the mouth is tilted dorsally at its anterior end, as reconstructed by Brazeau and de Winter (2015) and Davis *et al.* (2012), to some extent by Miles (1968, 1973) but not by Watson (1937) or Jarvik (1977).

Hyoid arch

The hyoid arch comprises paired hyomandibulae, interhyals, and ceratohyals, which join directly to a median basibranchial (Figs 2–4, 7, 8). The hyomandibula comprises a posterior and poorly mineralized anterior ossification (Fig. 8A, B; Miles 1968, 1973). The end of the hyomandibula contacting the neurocranium is laterally compressed in cross-section, meaning that overall the hyomandibula grades into a circular cross-section posteriorly, and the posterior part of the medial face of the hyomandibula is split by a marked, longitudinal ridge,

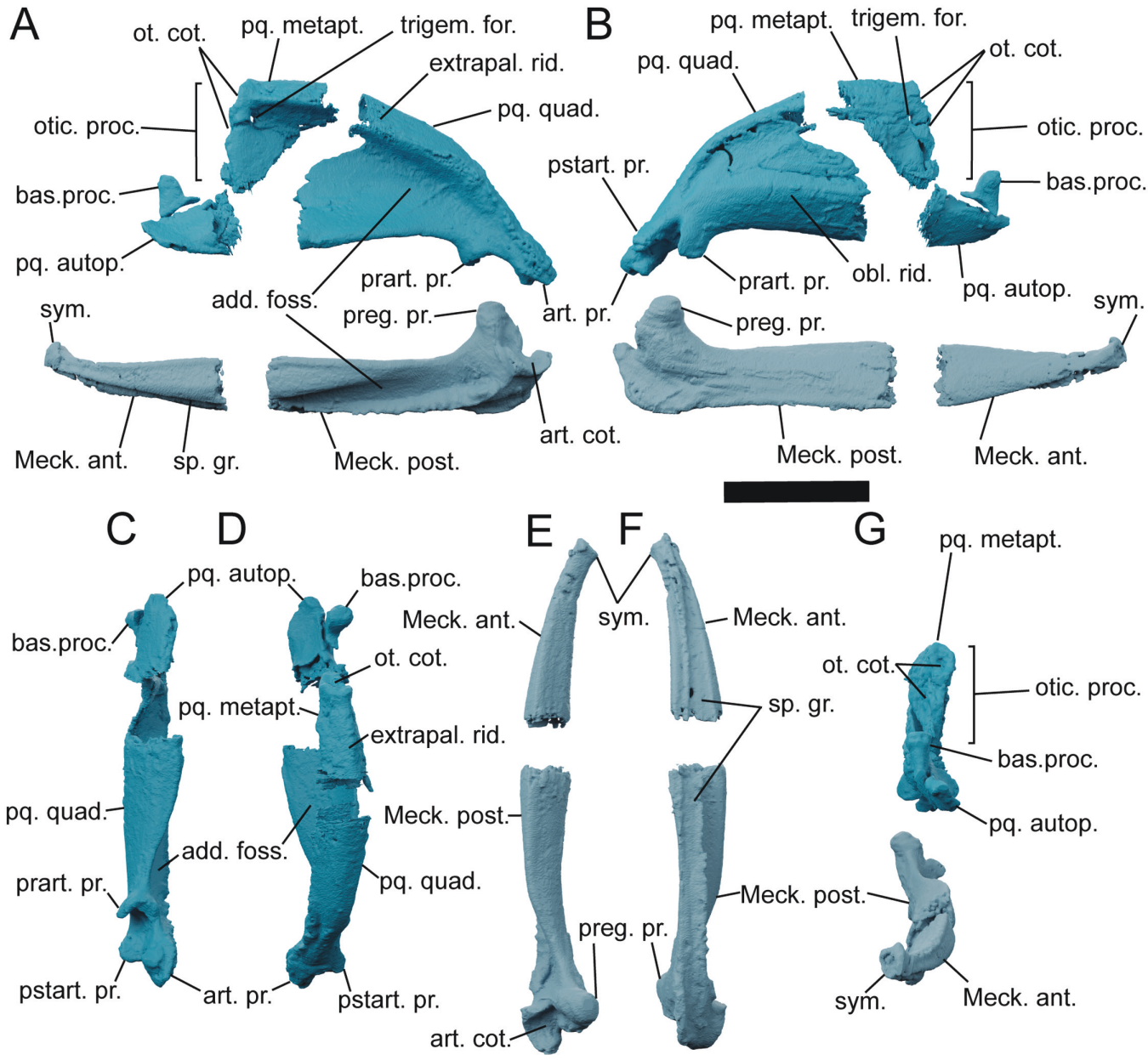

Figure 6. The mandibular arch of *Acanthodes confusus* MNHN-F-SAA21. A, left Meckel's cartilage and palatoquadrate in lateral view. B, left Meckel's cartilage and palatoquadrate in medial view. C, D, left palatoquadrate in (C) ventral and (D) dorsal view. E, F, left Meckel's cartilage in (E) dorsal and (F) ventral view. G, left Meckel's cartilage and palatoquadrate in anterior view. Abbreviations: add. foss., fossa for the adductor muscle; art. cot., articular cotylus; art. pr., articular process; bas. proc., basal process; extrapal. rid., extrapalatoquadrate ridge; Meck. ant., anterior mineralization of Meckel's cartilage; Meck. post., posterior mineralization of Meckel's cartilage; obl. rid., oblique ridge; ot. cot., cotylus for articulation with otic region; otic. proc., otic process; pq. autop., palatoquadrate autopalatine; pq. metapt., palatoquadrate metapterygoid; pq. quad., palatoquadrate quadrate; prart. pr., prearticular process; preg. pr., preglenoid process; sp. gr., mandibular splint groove; sym., expanded mandibular symphysis; trigem. for., foramen for the mandibular ramus of the trigeminal nerve (V_3). Scale bar = 20 mm.

which separates it into dorsomesial and ventromesial faces (Fig. 7F; Miles 1968). Miles (1968) drew a comparison between this shape and the hyomandibula of hexanchiform sharks. Amongst Palaeozoic forms the laterally flattened, curved, and posteriorly tapered shape of the hyomandibula is more comparable to that of the actinopterygian *Mimipiscis* (Gardiner 1984), the symmoriiforms *Ozarcus* (Pradel *et al.* 2014) and *Ferromirum* (Frey *et al.* 2020), and cladoselachians (Maisey 1989) than to the stem-group chondrichthyan *Gladbachus* (Coates *et al.* 2018) or to the stouter hyomandibulae of crown-group chondrichthyans such as xenacanths or hybodonts (Hotton 1952, Maisey 1987).

An interhyal is present between the hyomandibula and ceratohyal of *Acanthodes* (Figs 4, 7, 8A, B, G, H), confirming the account of Miles (1973). The interhyal is subrectangular and laterally flattened, with gently convex dorsal and ventral surfaces. Of the three specimens described here, interhyals are only preserved in MNHN-F-SAA24 (Fig. 4) and before that were only known from a single mouldic specimen, MFN MB 23, now lost but from which casts are preserved (e.g. NHMUK

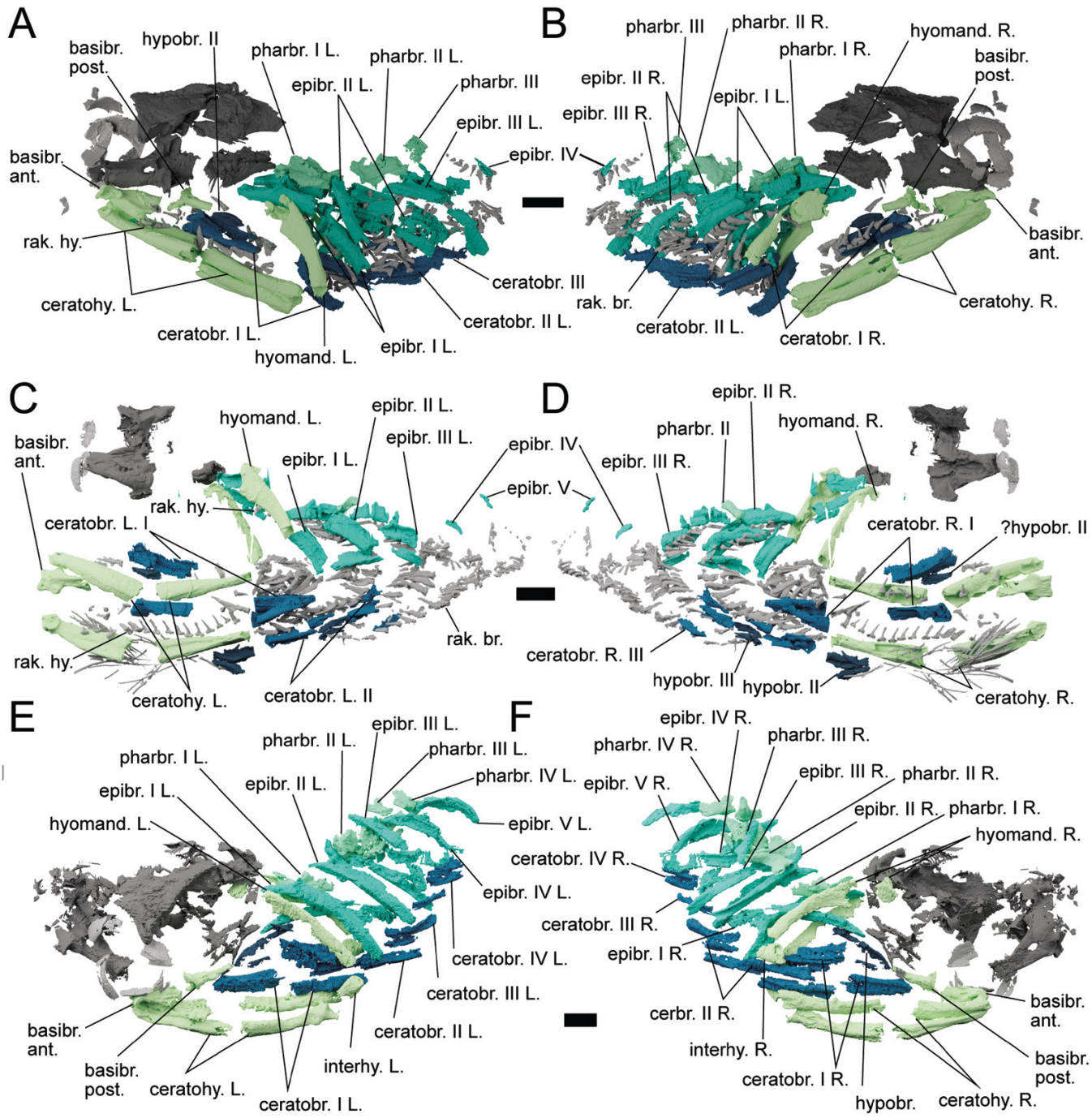

Figure 7. Overview of *Acanthodes confusus* hyoid and branchial skeleton. A, B, MNHN-F-SAA21 with mandibular skeleton removed in (A) left lateral and (B) right lateral view. C, D, MNHN-F-SAA20 with mandibular and pectoral skeleton removed in (C) left lateral and (D) right lateral view. E, F, MNHN-F-SAA24 with mandibular and pectoral skeleton removed in (E) left lateral and (F) right lateral view. Abbreviations: basibr., basibranchial; ceratobr., ceratobranchials; ceratohy., ceratohyal; epibr., epibranchial; hyomand., hyomandibula; interhy., interhyal; L., left; Meck., Meckel's cartilage; pharbr., pharyngobranchials; R., right; rak. br., branchial rakers; rak. hy., hyoid rakers. Colour scheme: blue-greens, elements of visceral endoskeleton with mandibular arch, hyoid arch, hypobranchials, ceratobranchials, epibranchials, and pharyngobranchials coloured independently; dark grey, cranial and pectoral endoskeleton; light grey, elements of the dermal skeleton. Scale bars = 10 mm.

PV P 49990, Miles 1973, plate 7). The proportions of the interhyal in MNHN-F-SAA24 relative to the hyomandibula approximately match those of the interhyal in NHM PV P 49990, which comparison suggests probably preserves a postero-lateral view of the element. As Miles (1973) highlighted it is unclear whether this 'interhyal' is homologous to the interhyal, stylohyal, or symplectic in osteichthyans (Patterson 1982, Véran 1988). Whether or not these are homologous, additional elements of the hyoid skeleton are not found in this position in *Gladbachus* (Coates *et al.* 2018), or in other articulated Palaeozoic chondrichthyan hyoid arches (Pradel *et al.* 2014, Frey *et al.* 2020, Klug *et al.* 2023).

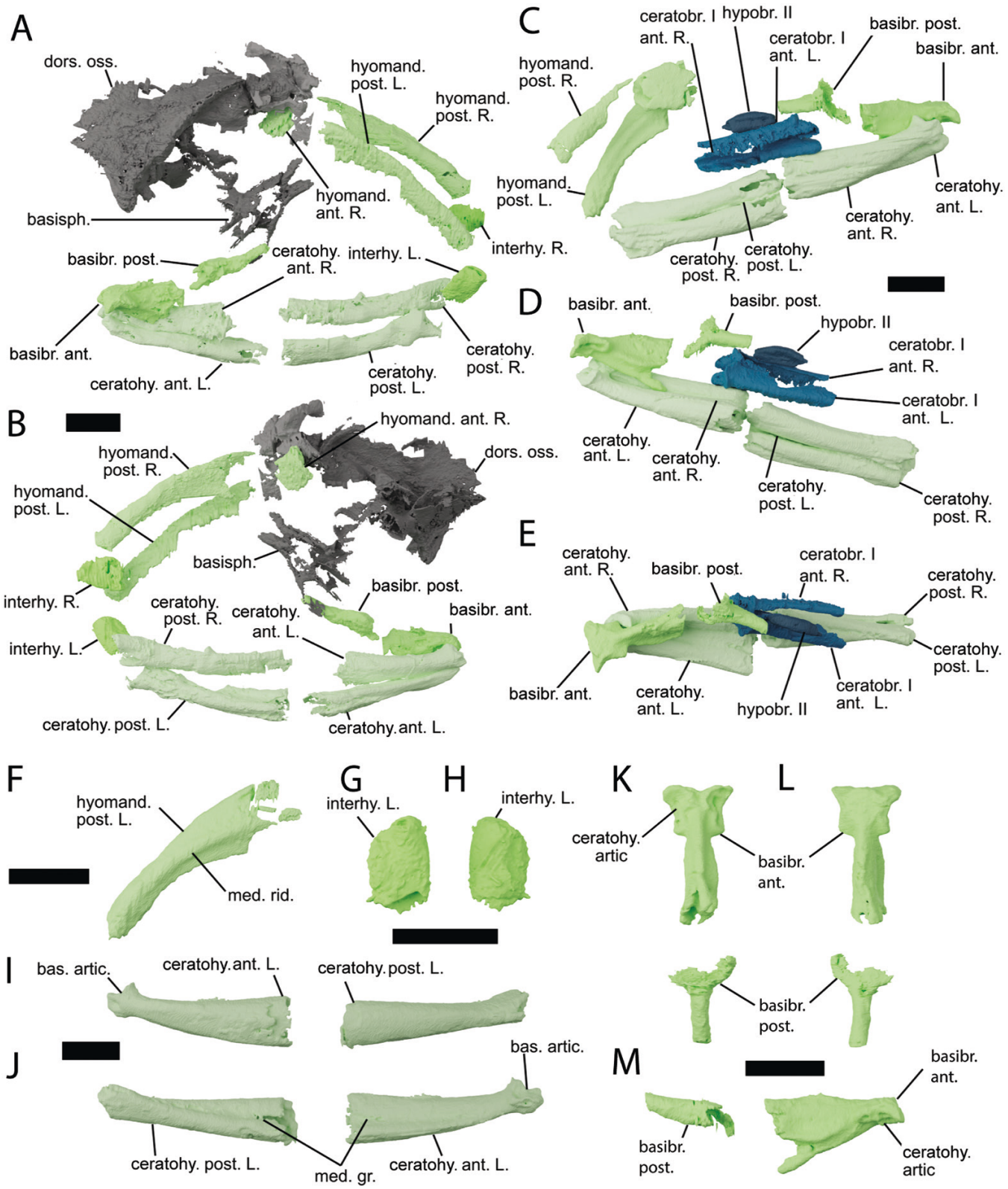

Figure 8. The hyoid skeleton of *Acanthodes confusus*. A, B, the hyoid skeleton of MNHN-F-SAA24 in (A) left lateral and (B) right lateral view. C–E, the hyoid skeleton of MNHN-F-SAA21 in (C) right lateral, (D) left lateral, and (E) dorsal view. F, the posterior mineralization of the left hyomandibula in MNHN-F-SAA21. G, H, the left interhyal of MNHN-F-SAA24 in (G) lateral and (H) medial view. I, J, the left ceratohyal of MNHN-F-SAA21 in (I) lateral and (J) medial view. K–M, the basibranchial of MNHN-F-SAA21 in (K) ventral, (L) dorsal, and (M) right lateral view. Abbreviations: ant., anterior ossification; artic., articulation; basibr., basibranchial; basisph., basisphenoid; ceratohy., ceratohyal; dors. oss., dorsal ossification of neurocranium; L., left; hyomand., hyomandibula; hypobr., hypobranchials; med. gr., medial groove; med. rid., medial ridge; post., posterior ossification; R., right.; I–II, branchial arches I–II. Scale bar = 10 mm.

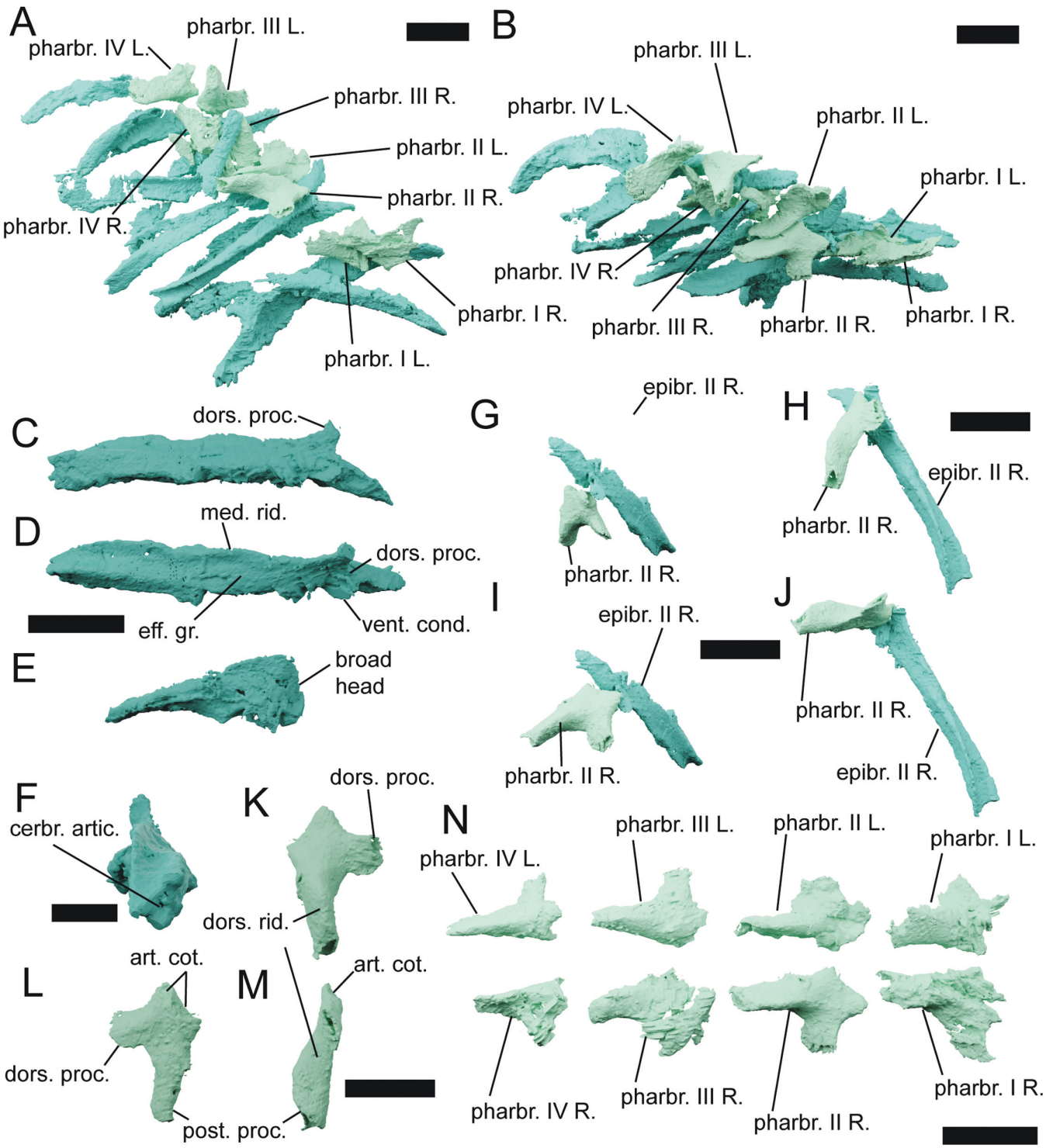

Figure 9. The dorsal branchial skeleton of *Acanthodes confusus*. A, B, articulated dorsal branchial skeleton of MNHN-F-SAA24 in right lateral (A) and dorsal (B) view with pharyngobranchials labelled. C–D, the right epibranchial II of MNHN-F-SAA24 in (C) lateral and (D) dorsal. E, the left fifth epibranchial of MNHN-F-SAA24 in dorsal view. F, the right epibranchial II of MNHN-F-SAA24 in posterior view. G, H, right epibranchial and pharyngobranchial II of MNHN-F-SAA24 as preserved in (G) dorsal and (H) posterior view. I, J, right epibranchial and pharyngobranchial II of MNHN-F-SAA24 repositioned into estimate of life position in (I) dorsal and (J) posterior view. K–M, the right pharyngobranchials II of MNHN-F-SAA24 in (K) dorsal, (L) ventral, and (M) lateral view. N, all pharyngobranchials from MNHN-F- SAA24 in dorsal view. Abbreviations: artic., articulation; art. cot., articular cotylus; cerbr., ceratobranchial; dors. proc., dorsal process; dors. rid., dorsal ridge; epibr., epibranchial; L., left; med. rid., medial ridge; pharbr., pharyngobranchial; post. proc., posterior process; R., right; vent. cond., ventral condyle; I–V, branchial arches I–V. Scale bar = 10 mm.

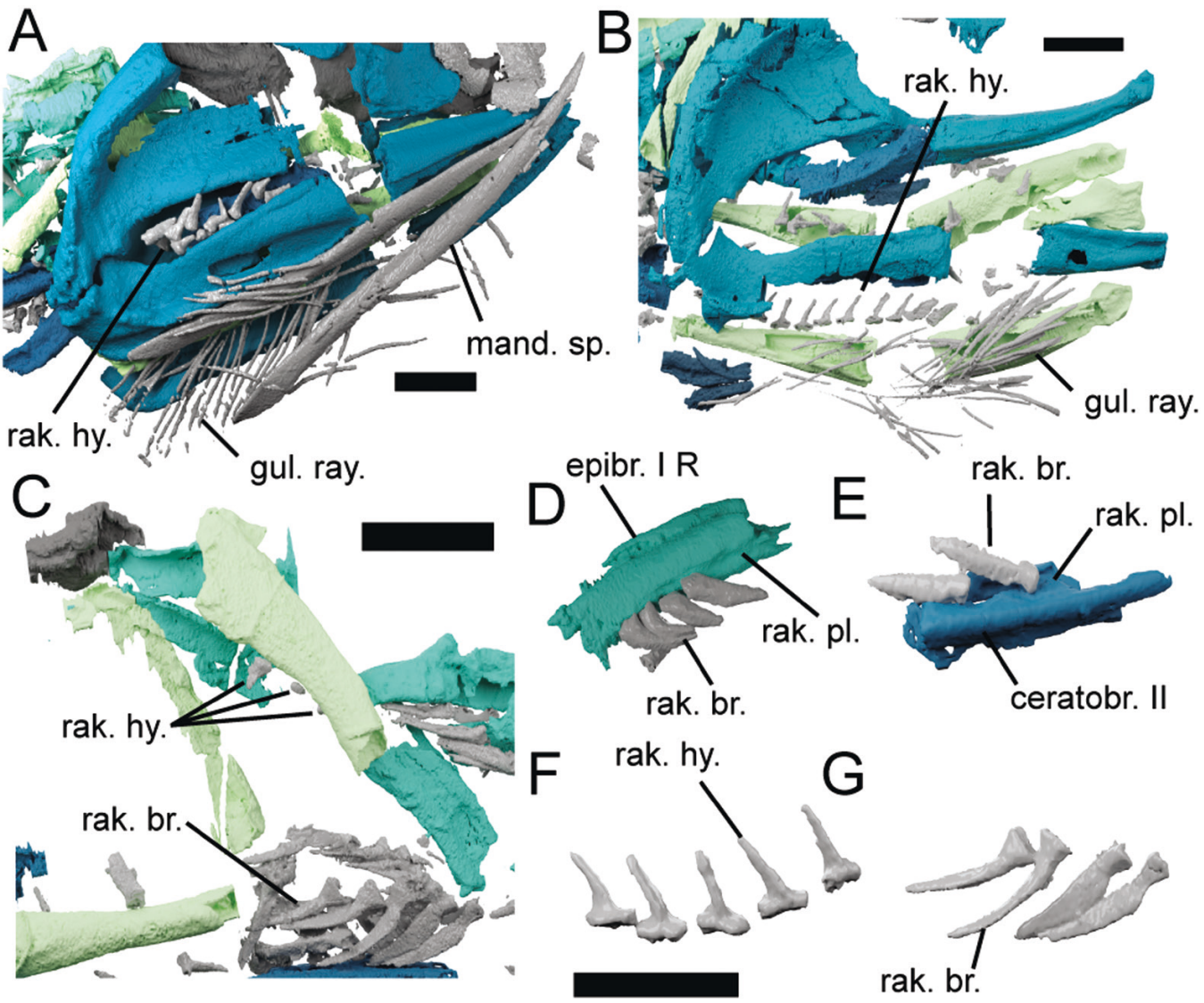

Figure 10. The gular rays, hyoid rakers, and branchial rakers of *Acanthodes confusus*. A, right lateral view of jaws of MNHN-F-SAA21 showing relationship of gular rays and mandibular splint to Meckel's cartilage. B, right lateral view of jaws of MNHN-F-SAA20 with mandibular splints removed showing gular rays and relationship of hyoid rakers to ceratobranchial. C, left lateral view of MNHN-F-SAA20 showing hyomandibular rakers. D, branchial rakers in articulation with the epibranchial of SAA21. E, branchial rakers in articulation with the ceratobranchial of SAA21. F, hyoid rakers from the ceratohyal of SAA20. G, branchial rakers from the epibranchial of SAA20. Abbreviations: ceratobr., ceratobranchials; epibr., epibranchial; gul. ray., gular rays; rak. br., branchial rakers; rak. hy., hyoid rakers; rak. pl., plinth for branchial raker; I–V, branchial arches I–V. Scale bar = 10 mm except in C where scale bar = 2.5 mm. Note in D and E the shape of the rakers is poorly captured by the scan.

The ceratohyal is ossified in two parts with no hypohyals present (Figs 2–4, 7, 8A–E, I, J; Miles 1965, 1968, 1973, Gardiner 1984) and its morphology confirms the account of Miles (1968). The posterior end is laterally flattened and lacks the lateral fossa seen in some early chondrichthyans (Coates *et al.* 2018). It also lacks the sharp dorsal angle at the posterior end of the ceratohyals of *Ferromirum* (Frey *et al.* 2020), *Phoebodus* (Frey *et al.* 2019), and *Maghriboselache* (Klug *et al.* 2023). The anterior end of the ceratohyal is not spatulate anteriorly like some Palaeozoic chondrichthyans such as *Phoebodus* (Frey *et al.* 2019), instead pinching in and expanding out to form the articulation with the basibranchial (the *expanded knob* of Miles 1968). The longitudinal groove runs along the mesial surface of the element which may be homologous to a similar groove on the ceratohyal of *Gydoselache* (Maisey *et al.* 2019) and which Miles (1968) suggested was for the insertion of muscles including the anterior interhyoideus musculature.

The component forming the ventral floor of the pharyngeal skeleton is composed of two mineralized parts (Figs 2–4, 7, 8A–E, K–M). This has variously been termed a basibranchial or basihyal; here we use the former due to its extending considerably further posteriorly than most elasmobranch basihyals. The anterior mineralization has a hammerhead-shaped anterior end with ventrally-oriented articulation surfaces for the ceratohyals. In its posterior half this becomes taller with deep ventral attachment surfaces for the coracohyoid and coracobranchial musculature, with an unfinished posterior face (i.e. not covered by perichondral bone). The posterior basibranchial mineralization is flat with a posterior tail, its unfinished anterior face suggests that it was joined to the anterior mineralization of the basibranchial

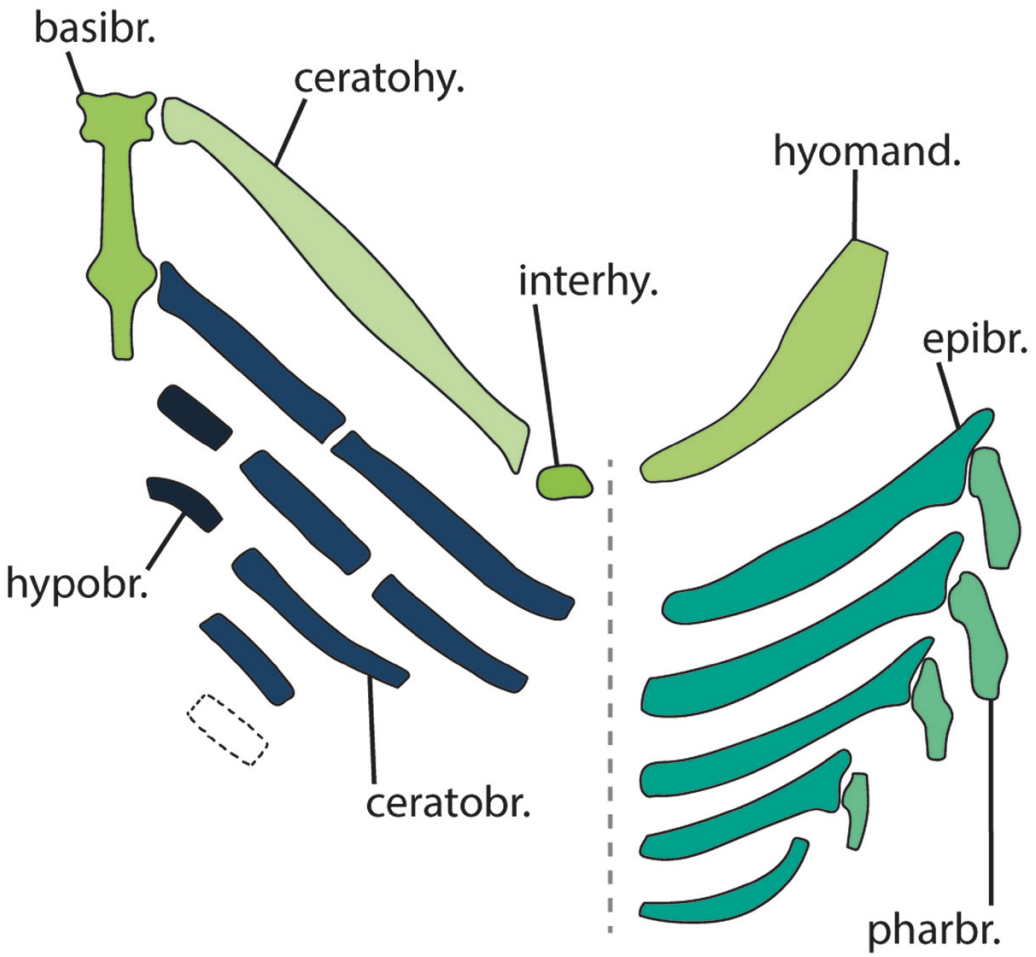

Figure 11. Reconstruction of the pharyngeal skeleton of *Acanthodes confusus* as described here. Abbreviations: basibr., basibranchial; ceratobr., ceratobranchials; ceratohy., ceratohyal; epibr., epibranchial; hyomand., hyomandibula; hypobr., hypobranchial; interhy., interhyal; pharbr., pharyngobranchials. Matching colours denote serially homologous elements. Reconstruction shown as if spread horizontally, with anterior above.

by cartilage. There are no obvious articulation surfaces on the posterior part of the basibranchial, but based on their preserved position it seems likely to have articulated with the first and second branchial arch as reconstructed by Miles (1973). This tall, narrow basibranchial is dissimilar from the broad flat basihyals of other known stem-group chondrichthyans (Brazeau 2012, Coates *et al.* 2018); a possible exception is in *Halimacanthodes*, where an element identified as an ?autopalatine (or possibly a basibranchial) could be the front of the basibranchial in lateral profile (Burrow *et al.* 2012). A tapering posterior end is common in basibranchial copulae in extant and extinct chondrichthyans (Coates *et al.* 2018, Dearden *et al.* 2021), although otherwise these are dissimilar from the basibranchial in *Acanthodes* in that copulae extend considerably beyond the posterior-most branchial arch (e.g. Dearden *et al.* 2021). We find no evidence for a chain of basibranchial elements as given in some reconstructions (Fig. 1A–C): this aspect of the reconstruction appears to be based on the holotype of *A. confusus* (Heidtke 2011: fig. 8) in which preserved hypobranchials give the impression of there having been a chain of basibranchials.

Branchial arches

Five branchial arches are preserved which extend well-posterior to the braincase (Figs 2–4, 7, 9). It remains unclear whether they articulated with the basioccipital, as reconstructed by Miles (1973). In MNHN-F-SAA21 they overlap with the underside of the braincase anteriorly (Fig. 2) but this is not the case in MNHN-F-SAA24 and MNHN-F-SAA20 [Figs 3, 4; see discussion of this character state in Dearden *et al.* (2019), Supplementary material, Character 50, of Frey *et al.* (2020)]. The branchial arches comprise hypo-, cerato-, epi-, and pharyngobranchials. We find no evidence for accessory elements as in some osteichthyans and in the symmoriiform *Ozarcus* (Pradel *et al.* 2014).

Four pairs of ceratobranchials are preserved, a fifth ceratobranchial is absent although rakers on the ventral part of the fifth arch in MNHN-F-SAA20 (Figs 3, 7C) indicate that there was a ventral component to the fifth branchial arch. The ceratobranchials all have a similar overall structure, with a ventral groove for the afferent branchial artery and plinths on their pharynx-facing surfaces for the branchial rakers (Fig. 7). Ceratobranchial I and II are segmented into anterior and posterior sections, and ceratobranchial I has a pronounced articular facet on its anterior end which must have articulated with the basibranchial, although there is no corresponding facet on that element. More posterior ceratobranchials become progressively shorter and more pronouncedly curved until the fourth pair is almost as broad as they are long (Fig. 7E, F). The posteriormost ceratobranchial is not enlarged as in *Gladbachus* and the stem-group gnathostome

Paraplesiobatis (Brazeau *et al.* 2017, Coates *et al.* 2018), yet is more flattened relative to the others as observed in these taxa.

Hypobranchials are present on at least the second and third branchial arches (Fig. 7). No hypobranchial IV is visible in our datasets (Fig. 7), although a cast of a now lost specimen (NHMUK PV P 49990; Miles 1973, plate 7) shows a hypobranchial in this position quite clearly that conforms with the anatomy of the more anterior hypobranchials so it may be either lost or unmineralized in the specimens studied here. The hypobranchials are short and curved, with a lateral groove, and are oriented anteriorly. Ceratobranchial I has a well-developed condyle at its anterior tip and is preserved in close association with the basibranchial in MNHN-F-SAA21 (Fig. 8C, D), suggesting a direct connection between the two without an intervening hypobranchial. We find no evidence for a fifth hypobranchial.

Five pairs of epibranchials are present, one in each arch (Figs 7, 9). The epibranchials are gently curved, with a dorsolateral groove for the efferent branchial artery (Fig. 9A, B). This groove is bordered medially by a ridge corresponding to the posterior flange (Coates *et al.* 2018). At the distal end of the ceratobranchial this develops into a dorsal process (Miles 1968). Like the ceratobranchials the surface facing into the branchial chamber is pitted forming a series of plinths to carry the gill rakers (Fig. 10E). The proximal end of the epibranchials has an articular surface for the ceratobranchial (Fig. 9C). The epibranchials have the same overall form, but become progressively shorter posteriorly (Figs 7, 9H). The posteriormost (fifth) epibranchials are different in shape, with broad heads (Figs 7, 9E). Although the epibranchials in MNHN-F-SAA20 and MNHN-F-SAA21 appear to be segmented, in MNHN-F-SAA24 they are ossified into a single structure (Figs 4, 9).

There are four pairs of pharyngobranchials, best preserved in MNHN-F-SAA24 (Figs 4, 7, 9) where all four pairs are preserved in articulation with the epibranchials. The individual anatomy of these pharyngobranchials is consistent with the description of Miles and that observed in casts of mouldic specimens (e.g. NHMUK PV P 59959, Miles 1973: pl. 2), and there is no evidence for separate supra- and infrapharyngobranchials as in *Ozarcus* and osteichthyans (Gardiner 1984, Pradel *et al.* 2014). The morphology of each successive pair of pharyngobranchials is serially consistent, although the more posterior pharyngobranchials are slightly smaller. Unlike living chondrichthyans, but like *Gladbachus* and *Ptomacanthus* (Coates *et al.* 2018, Dearden *et al.* 2019) the posteriormost epibranchials and pharyngobranchials are not fused into a single complex element. The only other acanthodiform in which pharyngobranchials have been figured is *Halimacanthodes*, in which they appear broadly similar in shape (Burrow *et al.* 2012: fig. 2b, *ph. br.*).

The articulation between each pharyngobranchial and the head of each epibranchial confirms the account of Miles (1973), with two cotyli on the anterior end of each pharyngobranchial fitting with two condyli on the head of each ceratobranchial. This articulation is preserved *in situ* in the right, second branchial arch of MNHN-F-SAA24 (Fig. 9G–J), and the positions of the other pharyngobranchials in this specimen are consistent with the same articulation. Nelson (1968) outlined two alternative arrangements of the pharyngobranchials in *Acanthodes* (Fig. 1C): one where each pharyngobranchial was oriented anteriorly from the more posterior arch to meet the one in front, and another where pharyngobranchials were oriented posteromedially from the top of each arch. Reconstructing the articulation between this pharyngobranchial and epibranchial leads to an angle of about 90 ° between the two, suggesting that the latter of Nelson's reconstructions is accurate (Figs 9I, J, 12). Moreover there is no visible articulatory surface on the posterior end of each pharyngobranchial (Fig. 9K, N), with them instead being narrow and unfinished (Miles 1973). Based on this we interpret these new data as confirming that *Acanthodes* had postero-medially oriented pharyngobranchials. The effect of the posterior process and dorsal ridge on each pharyngobranchial (Fig. 12) is thus to form a concave surface on the dorsal face each serving as anchoring points for the m. interpharyngobranchialis (Jarvik 1977).

HYOID AND BRANCHIAL RAKERS

Branchial and hyoid arches carry rows of small rakers. Our data is insufficiently high resolution to show any histological detail, but these elements are separate from the endoskeletal arches, with distinct bases and crowns, and are ornamented (Zidek 1985) so we consider it probable they are dermal rakers (Miles 1968) rather than endoskeletal projections from the pharyngeal arches (Ørvig 1973, Jarvik 1977). On the basis of MNHN-F-SAA21 and MNHN-F-SAA20 (Figs 2, 3) there is a single row of anteromedially directed rakers on each branchial arch, although more than one row on each arch has been reported, which may vary through ontogeny (Reis 1896, Watson 1937, Miles 1968). Some small rakers are present on the ventral part of the hyomandibula in MNHN-F-SAA20 (Reis 1896, Watson 1937, Miles 1968), and the ceratohyals carry a single row of rakers (Figs 2, 3, 7). Rakers are present on the dorsal and ventral parts of all five branchial arches, as can be seen in MNHN-F-SAA20 (Fig. 7C, D). They are positioned on plinths along the length of the branchial elements (Fig. 10).

The morphology of the rakers is variable on different elements (Fig. 10). On the ceratohyal and hyomandibula the rakers comprise simple prongs with a broad, flat base (Fig. 9I), and on the hyomandibula these are even simpler and smaller (Fig. 10C). Contrastingly, on the epibranchials and ceratobranchials the blade of each raker is considerably longer and developed into a flattened leaf shape slightly inflected away from the midline, and a base that is quite rounded and concave. These branchial rakers are larger on more anterior arches, and also decrease in size towards the top and bottom of either arch (Fig. 7C, D). More detailed views of raker morphology can be seen in casts, notably NHMUK PV P 49973 and 49990 (Miles 1973: pls 6, 7).

HYOID/GULAR RAYS

The hyoid/gular rays are preserved in all three specimens, although the lateral collapse of the skeleton in each case has disarticulated them to some extent (Figs 1–3, 10A, B). They are short narrow elements, some of which having a slight sinusoidal inflection (Dearden and Giles 2021). They are oriented posteromedially from the ventral margin of each mandible [this can be clearly seen in NHMUK PV P 49973 (Miles 1973: pl.

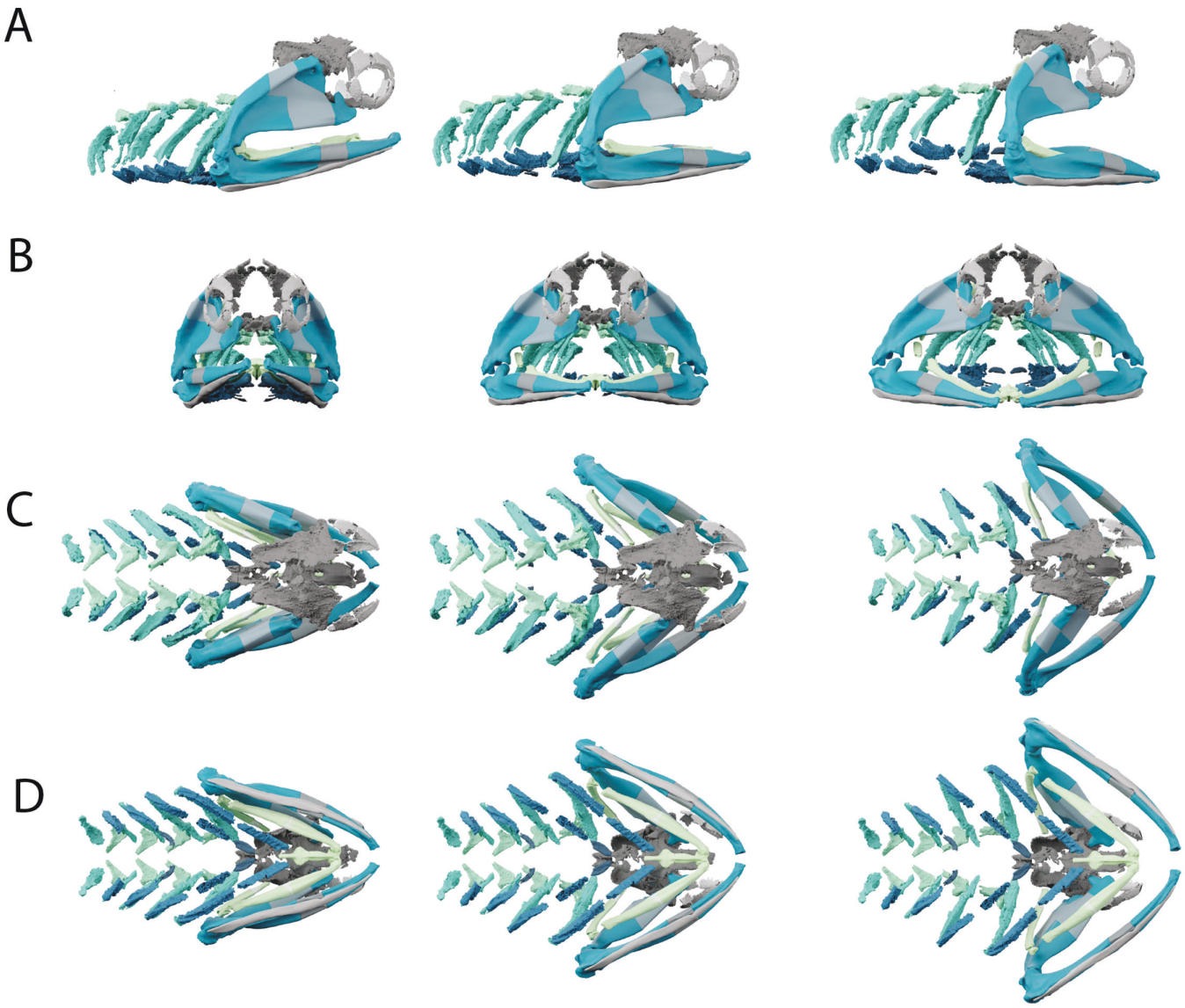

Figure 12. Reconstruction of *Acanthodes confusus* based on a composite of the material described here, animated to show mouth opening from left to right. A, in right lateral view. B, in anterior view. C, in dorsal view. D, in ventral view.

6)], and appear to be absent from the first fifth of the mandible's length and then be arranged into a row running just beyond the mandible's posterior margin. In life they would have underlain the gular region.

FUNCTIONAL MORPHOLOGY

Our 3D reconstruction confirms that the reconstruction of Miles (1968) with three points of articulation with the neurocranium is plausible (Fig. 12) and that the effect of swinging the jaw laterally from these articulatory points is that the palatoquadrates swing laterally as he predicted. The double articulation of the Meckel's cartilage and the palatoquadrate means that the mandible could only lower vertically relative to the palatoquadrate (Miles 1968); as such the relative angles of the left and right mandibles change during jaw opening. This is perhaps the reason for the expanded symphyseal tip on the mandible, to accommodate the connective tissue (ligaments, cartilage) that allows this movement. Another effect of this movement is that the symphysis of the mandible moves anteriorly during jaw opening (Fig. 12). Our reconstruction suggests the proximal end of the hyomandibula would have been capable of staying close to the jaw articulation even with major abduction of the palatoquadrate. We note that we did not place any constraints on movement beyond the direction of rotation, so this reconstruction should be interpreted as a plausible rather than a maximum gape. Moreover, it is likely that in life the unmineralized cartilaginous midsections of the jaws and hyoid arch would have given them some degree of flexibility, something that is not incorporated into our model.

DISCUSSION

Pharyngeal skeletal patterning in *Acanthodes*

Our CT data allow us to arbitrate between previous reconstructions (Fig. 11) and place this anatomy in the context of recent advances in our understanding of Palaeozoic gnathostome pharyngeal anatomy. Several reconstructions of the pharyngeal

endoskeleton of *Acanthodes confusus* have been made based exclusively on casts of fossils from Lebach (Fig. 1). Early reconstructions were made by Reis (1890, 1894, 1895, 1896) and then by Dean (1907). Watson (1937) then reconstructed the skeleton and used it as the basis for his argument that acanthodians were aphetohyoidean. Renewed interest in the late 20th century then led to reconstructions by Miles (1964, 1968, 1973), Nelson (1968), Jarvik (1977), and Gardiner (1984). Since then no new information on the branchial skeleton has been published although the branchial skeleton has been discussed by Coates *et al.* (2018), Dearden *et al.* (2019), and Davis *et al.* (2012), and Brazeau and de Winter (2015) reassessed the articulation of the hyomandibula with the braincase. Disagreement between these reconstructions centres around the presence/absence of hyoid components (interhyal, pharyngohyal, and hypohyal), the structure of the basihyal/branchial skeleton, and the orientation of any hypobranchials and pharyngobranchials, much of it caused by the segmentation of the pharyngeal skeleton (Fig. 1). Generally speaking the most recent reconstructions by Miles (1964, 1968, 1973), Gardiner (1984), and Nelson (1968) are the most accurate, with them correctly identifying which borders represent the unmineralized sections of elements.

Phylogenetic characters based on the branchial skeleton are necessarily based on interpreting the presence/absence of small, often-poorly mineralized components of a delicate skeletal structure. The multiple specimens of *Acanthodes* that we scanned, as well as other acid-prepared specimens, show how this fact combined with taphonomy can alter the interpretation of character states. For example, the interhyal is preserved in only one of the three specimens of *Acanthodes* we scanned, and in only one other specimen besides. Each epibranchial is preserved as a single unit in MNHN-F-SAA24 but is segmented in the other two specimens. Finally, a fifth ceratobranchial is implied by the presence of a fifth, ventral set of branchial rakers but is absent in all specimens. Mineralization of these elements may be influenced by factors such as ontogeny, although all specimens are approximately the same size, as estimated from their mandibles which are approximately 60 mm in length. Thus, caution should be taken in designing and coding pharyngeal characters based on presence/absence in a single specimen.

Osteichthyan and chondrichthyan pharyngeal character states

The pharyngeal skeleton of *Acanthodes* displays a combination of osteichthyan-like and chondrichthyan-like characters. Past interpretations of the pharyngeal anatomy of *Acanthodes* have varied between chondrichthyan-like (Jarvik 1977) and osteichthyan-like (Miles 1973) models. Recent studies of the neurocranial anatomy of *Acanthodes* have identified chondrichthyan-like characters such as a dorsal otic ridge (Davis *et al.* 2012) and a hyomandibular articulation ventral to the jugular vein (Brazeau and de Winter 2015), which form a major part of the evidence that *Acanthodes* is a stem-group chondrichthyan (Zhu *et al.* 2013, Coates *et al.* 2018, Dearden *et al.* 2019). However, the neurocranium also has several osteichthyan-like traits, inferred to be gnathostome crown-group symplesiomorphies, including spiracular grooves on the basisphenoid and a tropibasic neurocranium (Friedman and Brazeau 2010). Similarly, the branchial skeleton shows a combination of osteichthyan-like and chondrichthyan-like traits, although these are more difficult to polarize than cranial characters due to the dearth of information on the pharyngeal skeleton of stem-group gnathostomes (Carr *et al.* 2009, Brazeau *et al.* 2017). Here we discuss these based on the assumption that *Acanthodes* is indeed a stem-group chondrichthyan.

In terms of proportions the pharyngeal skeleton is rather osteichthyan-like. In the stem-group chondrichthyans *Ptomacanthus* and *Gladbachus*, as well as many extant elasmobranchs, the basihyal, and thus the pharyngeal floor, is broad with widely spaced ceratohyals (Coates *et al.* 2018, Dearden *et al.* 2019, 2021). In *Acanthodes* the basibranchial is narrow and the ceratohyals almost meet below its anterior end. This bears comparison with the arrangement in Palaeozoic actinopterygians where the hyoid arch (albeit with hypohyals) articulates closely together with the antero-ventral surface of a narrow basibranchial (Gardiner 1984, Giles *et al.* 2015). However, it is also comparable to the narrow-based pharynx of the symmoriiform *Ozarcus* (Pradel *et al.* 2014). Like *Ozarcus* and actinopterygians, *Acanthodes* has a narrow-based neurocranium and it is possible that these characters are functionally linked to a narrow pharynx and perhaps to other characters such as a flattened, slender hyomandibula rather than being phylogenetically informative.

The construction of the hyoid arch in *Acanthodes* is similar in arrangement to that of other stem-group chondrichthyans in which it is known, like *Gladbachus* and *Ptomacanthus*, in that a separate hypohyal andpharyngohyal are absent, and a basihyal/branchial is present (Coates *et al.* 2018, Dearden *et al.* 2019). However, an interhyal is absent in both of these other taxa and is demonstrably absent in the vast majority of other chondrichthyans in which the hyoid skeleton is known such as *Gladbachus*, *Tristychius*, and *Ozarcus* (Pradel *et al.* 2014, Coates *et al.* 2018, 2019). A possible interhyal reported in a cladoselachian (Maisey 1989) instead appears to represent the broken proximal end of the ceratohyal, split through the external fossa that is a common feature of Palaeozoic chondrichthyan ceratohyals (Coates *et al.* 2018). Amongst acanthodians an interhyal has also been reported in a specimen of *Ischnacanthus* (Brazeau and de Winter 2015) and an 'interhyal gap' (*interhyaler Spalt*) was identified in *Latviacanthus*, although without direct evidence of an interhyal's presence (Schultze and Zidek 1982).

One or more skeletal elements between the ceratohyal and hyomandibula are present in osteichthyans, variously termed the interhyal, symplectic, and stylohyal, and have been cited as a character grouping them to the exclusion of chondrichthyans (Schaeffer 1968, Patterson 1982, Véran 1988). Similarities were recently drawn between the osteichthyan interhyal and a cartilage in a stem-group gnathostome buchanosteid (Hu *et al.* 2017). Which, if any, of the osteichthyan hyoid elements the interhyal in *Acanthodes* is homologous with is unclear and ultimately obscured by a poor understanding of hyoid arch morphology in stem-group gnathostomes and Palaeozoic osteichthyans (Véran 1988, Friedman and Brazeau 2010). Whatever the homology of the interhyal in *Acanthodes* the presence of a separate element between the ceratohyal and hyomandibula in *Acanthodes*, osteichthyans, and a stem-group gnathostome buchanosteid suggests that this may be a crown-group gnathostome symplesiomorphy.

Discussion of the pharyngobranchials in *Acanthodes* has in the past been framed in the context of contrasting states in living gnathostomes: anteriorly oriented infrapharyngobranchials and suprapharyngobranchials in osteichthyans vs. posteriorly oriented pharyngobranchials (assumed to be homologous to infrapharyngobranchials) in chondrichthyans (Nelson 1968, Miles 1973, Pradel *et al.* 2014). Our reconstruction confirms that *Acanthodes* was chondrichthyan-like in both respects. Recent descriptions of Palaeozoic chondrichthyan pharynxes based on computed tomography show that there is substantially more anatomical variation than might be expected from modern taxa. *Gladbachus* has anteriorly oriented pharyngobranchials with no suprapharyngobranchials (Coates *et al.* 2018), *Ptomacanthus* has a chain of pharyngobranchials that seem to span branchial arches (Dearden *et al.* 2019), and *Ozarcus* has anteriorly oriented infrapharyngobranchials that span branchial arches in addition to suprapharyngobranchials (Pradel *et al.* 2014).

Moreover, while the pharyngobranchials are posteriorly oriented in *Acanthodes*, they lack the long, flat swept-back blade that is present in living elasmobranchs and holocephalans (Pradel *et al.* 2014, Dearden *et al.* 2019). Coates *et al.* (2018) attempted to reconcile some of these morphologies by drawing comparison between the posteriorly directed crest articulating with the posterior arch in *Gladbachus* and that in *Acanthodes*. Our reconstruction suggests that this this is not the case in *Acanthodes*. However, if the ridged posterior processes on the pharyngobranchials of *Gladbachus* were oriented posteromedially instead of posteriorly to contact the arch behind (Coates *et al.* 2018: fig. S7), their anatomy could be reconciled with that of *Acanthodes*, albeit with a large, flat flange oriented antero-medially rather than the postero-laterally oriented dorsal process of *Acanthodes*. This could reflect the requirement in *Gladbachus* to support a broad pharyngeal roof. More generally the infrapharyngobranchials of *Ozarcus*, the pharyngobranchials of *Gladbachus*, and the pharyngobranchials of *Ptomacanthus* are similar to the pharyngobranchials of *Acanthodes* in the broad sense that there a longitudinal ridge runs over their dorsal surface.

Functional anatomy of the jaw

The most detailed previous study of the functional morphology of the jaws of *Acanthodes* jaws was by Miles (1968). Miles argued that the palatoquadrate was capable of extensive lateral abduction around the well-developed articulation points with the neurocranium. He considered this abduction to be most likely to be facilitated by the lateral movement of the hyoid bar, analogously to Palaeozoic actinopterygians (Schaeffer and Rosen 1961), although considered it unlikely that the hyomandibula played a major role in the jaw suspension itself, drawing analogy with hexanchiform sharks. He linked this to the suspension feeding mode of life that is commonly inferred for *Acanthodes* on the basis of its lack of teeth and numerous pharyngeal rakers.

Our reconstruction is broadly confirmatory of the proposal of Miles (1968) in that the palatoquadrates are able to rotate laterally significantly around the points of articulation with the neurocranium. Miles also suggested that the hyoid arch was the mechanism for pushing the jaws outwards. In living teleosts lateral movements are mainly caused passively by movement by the hypaxial and epaxial musculature (Muller 1989, Aerts 1991, Van Wassenbergh *et al.* 2013, Camp and Brainerd 2014). Miles cited the very well-developed articulatory surfaces between the ceratohyals and basibranchial and on the first ceratobranchials as evidence for this. We note there are also large areas for muscle attachment on the basibranchial suggesting that the basibranchial played an active role in pharyngeal function. Two functional constraints on this movement are the distance of the mandibular tips from one another and the distance of the middle of the hyoid arch from the back of the mandibular arch, assuming a mandibulo-hyoid ligament connected the two. In either case the degree to which this was restrictive is dependent on an unknowable connective tissue connection; however, our models suggests that the 30° abduction proposed by Miles is unlikely to have been possible. We note that the if the maximum angle of the palatoquadrate was less than 30° it would allow a greater degree of mandibular abduction, as the anterior tips of the jaws do not move as far apart when abducting.

The Mid-Late Palaeozoic saw the evolution of diverse specialized feeding strategies in chondrichthyans. These include suction feeders (Coates *et al.* 2019, Dearden *et al.* 2023), grasping arrangements (Frey *et al.* 2020), and nektonic suspension feeders (Coates *et al.* 2018). Although they foreshadow some modern elasmobranch feeding strategies, these all pre-date the evolution of the specialized jaw suspensions upon which diverse modern elasmobranch feeding strategies are based (Maisey 1980). In the ecological context of the Late Palaeozoic *Acanthodes* is part of a wider trend towards the evolution of eel-like body shapes in a phylogenetically diverse range of fishes (Stack *et al.* 2020). Increasing the gape laterally may have been particularly important due to the anguilliform body shape of *Acanthodes* giving it a comparatively small head-on profile relative to its body size. Although *Acanthodes confusus* is Permian, its skeleton is almost identical to taxa from the Middle Devonian (Burrow *et al.* 2009, 2012). This includes aspects of the mandibular apparatus: the expanded anterior end of the Meckel's cartilage appears to be present in *Halimacanthodes* (Burrow *et al.* 2012, Dearden and Giles 2021), while a double-faceted palatoquadrate has been reported in *Cheiracanthus* (Miles 1973). Although *Acanthodes confusus* is often characterized as the last gasp of the doomed acanthodians, it is perhaps more accurately framed as the last member of a 100-million-year-old lineage with a remarkably resilient body plan incorporating an innovative feeding mechanism.

SUPPORTING INFORMATION

Supplementary data is available at *Zoological Journal of the Linnean Society* online.

ACKNOWLEDGEMENTS

We would like to thank the three anonymous referees for their helpful and constructive comments on the manuscript. Many thanks to Nathalie Poulet-Crovisier and Florent Goussard (MNHN CR2P) for help with 3D segmentation and visualization. Thanks also to Marta Bellato and Patricia Wils help with to X-ray Tomography (AST-RX platform UMS 2700 2AD CNRS-MNHN, Paris).

CREDIT STATEMENT

Richard P. Dearden (Conceptualization, Investigation, Data Curation, Writing—Original Draft, Writing—Review & Editing, Visualization, Funding acquisition), Anthony Herrel (Conceptualization, Writing—Review & Editing, Funding acquisition) and Alan Pradel (Conceptualization, Investigation, Writing—Review & Editing, Funding acquisition)

CONFLICT OF INTEREST

The authors declare no conflict of interest.

FUNDING

This work was funded by a Paris Île-de-France Region grant [Domaine d'intérêt majeur (DIM) 'Matériaux anciens et patrimoniaux'] awarded for the DIM PHARE (Pharyngeal Evolution: illuminating its function in early jawed vertebrates) project. R.P.D. is now supported by the European Union Horizon Europe programme on Marie Skłodowska-Curie Action DEADSharks (grant agreement number 101062426). A.P. is supported by the Agence nationale de la recherche (grant CE02) Terre vivante, jeunes chercheurs ou des jeunes chercheuses, ANR-22-CE02-0015-01_MACHER.

DATA AVAILABILITY

The CT data underlying this study are publicly available via MorphoSource at the following links: MNHN-F-SAA20 (https://doi.org/10.17602/M2/M569004), MNHN-F-SAA21 (https://doi.org/10.17602/M2/M568233), and MNHN-F-SAA24 (https://doi.org/10.17602/M2/M568946). 3D models are freely available via MorphoMuseuM (Dearden *et al.* 2024).

REFERENCES

Aerts P. Hyoid morphology and movements relative to abducting forces during feeding in *Astatotilapia elegans* (Teleostei: Cichlidae). *Journal of Morphology* 1991;**208**:323–45. https://doi.org/10.1002/jmor.1052080308

Bishop PJ, Cuff AR, Hutchinson JR. How to build a dinosaur: MUSCLOSKELETAL modeling and simulation of locomotor biomechanics in extinct animals. *Paleobiology* 2021;**47**:1–38.

Brazeau MD. A revision of the anatomy of the Early Devonian jawed vertebrate *Ptomacanthus anglicus* Miles. *Palaeontology* 2012;**55**:355–67. https://doi.org/10.1111/j.1475-4983.2012.01130.x

Brazeau MD, de Winter V. The hyoid arch and braincase anatomy of *Acanthodes* support chondrichthyan affinity of 'acanthodians'. *Proceedings of the Royal Society B: Biological Sciences* 2015;**282**:20152210. https://doi.org/10.1098/rspb.2015.2210

Brazeau MD, Friedman M, Jerve A *et al.* A three-dimensional placoderm (stem-group gnathostome) pharyngeal skeleton and its implications for primitive gnathostome pharyngeal architecture. *Journal of Morphology* 2017;**278**:1–9.

Burrow CJ, Blaauwen JLD. Endoskeletal tissues of acanthodians (stem Chondrichthyes). In: Pradel A, Denton JSS, Janvier P (eds), *Ancient Fishes and their Living Relatives: A Tribute to John G. Maisey.* Munich, Germany: Verlag Dr. Friedrich Pfeil, 2021, 81–91.

Burrow CJ, Blaauwen JD, Newman M. A redescription of the three longest-known species of the acanthodian *Cheiracanthus* from the Middle Devonian of Scotland. *Palaeontologia Electronica* 2020;**23**:1–43.

Burrow CJ, Long JA, Trinajstic K. Disarticulated acanthodian and chondrichthyan remains from the Upper Middle Devonian Aztec Siltstone, southern Victoria Land, Antarctica. *Antarctic Science* 2009;**21**:71–88. https://doi.org/10.1017/s0954102008001521

Burrow CJ, Newman MJ, den Blaauwen J *et al.* The Early Devonian ischnacanthiform acanthodian *Ischnacanthus gracilis* (Egerton, 1861) from the Midland Valley of Scotland. *Acta Geologica Polonica* 2018;**68**:335–62.

Burrow CJ, Trinajstic K, Long JA. First acanthodian from the Upper Devonian (Frasnian) Gogo Formation, Western Australia. *Historical Biology* 2012;**24**:349–57. https://doi.org/10.1080/08912963.2012.660150

Camp A, Brainerd EL. Role of axial muscles in powering mouth expansion during suction feeding in largemouth bass (*Micropterus salmoides*). *Journal of Experimental Biology* 2014;**217**:8.

Carr R, Johanson Z, Ritchie A. The phyllolepid placoderm *Cowralepis mclachlani*: insights into the evolution of feeding mechanisms in jawed vertebrates. *Journal of Morphology* 2009;**270**:775–804.

Coates MI, Finarelli JA, Sansom IJ *et al.* An early chondrichthyan and the evolutionary assembly of a shark body plan. *Proceedings of the Royal Society B: Biological Sciences* 2018;**285**:1–10.

Coates MI, Tietjen K, Olsen AM *et al.* High-performance suction feeding in an early elasmobranch. *Science Advances* 2019;**5**:eaax2742. https://doi.org/10.1126/sciadv.aax2742

Coates MI, Tietjen K, Johanson Z, Friedman M, Sang S. The cranium of *Helodus simplex* (Agassiz, 1838) revised. In: Pradel A, Denton JSS, Janvier P (eds), *Ancient Fishes and their Living Relatives: A Tribute to John G. Maisey*. Munich: Verlag Dr. Friedrich Pfeil, 2021, 193–205.

Davis SP, Finarelli JA, Coates MI. Acanthodes and shark-like conditions in the last common ancestor of modern gnathostomes. *Nature* 2012;**486**:247–50. https://doi.org/10.1038/nature11080

Dean BYB. Notes on acanthodian sharks. *American Journal of Anatomy* 1907;**7**:209–26. https://doi.org/10.1002/aja.1000070204

Dearden RP, Giles S. Diverse stem-chondrichthyan oral structures and evidence for an independently acquired acanthodid dentition. *Royal Society Open Science* 2021;**8**:210822. https://doi.org/10.1098/rsos.210822

Dearden RP, Herrel A, Pradel A. Evidence for high-performance suction feeding in the Pennsylvanian stem-group holocephalan *Iniopera*. *Proceedings of the National Academy of Sciences of the United States of America* 2023;**120**:1–8.

Dearden RP, Herrel A, Pradel P. 3D models related to the publication: the pharynx of the iconic stem-group chondrichthyan *Acanthodes* Agassiz, 1833 revisited with micro computed tomography. *MorphoMuseuM* 2024:e226. https://doi.org/10.18563/journal.m3.226

Dearden RP, Mansuit R, Cuckovic A *et al.* The morphology and evolution of chondrichthyan cranial muscles: a digital dissection of the elephantfish *Callorhinchus milii* and the catshark *Scyliorhinus canicula*. *Journal of Anatomy* 2021;**238**:1082–105. https://doi.org/10.1111/joa.13362

Dearden RP, Stockey C, Brazeau MD. The pharynx of the stem-chondrichthyan *Ptomacanthus* and the early evolution of the gnathostome gill skeleton. *Nature Communications* 2019;**10**:1–7.

Frey L, Coates MI, Ginter M, *et al.* The early elasmobranch *Phoebodus*: phylogenetic relationships, ecomorphology and a new time-scale for shark evolution. *Proceedings of the Royal Society B: Biological Sciences* 2019;**286**:20191336. https://doi.org/10.1098/rspb.2019.1336

Frey L, Coates MI, Tietjen K *et al.* A symmoriiform from the Late Devonian of Morocco demonstrates a derived jaw function in ancient chondrichthyans. *Communications Biology* 2020;**3**:1–10.

Friedman M, Brazeau MD. A reappraisal of the origin and basal radiation of the Osteichthyes. *Journal of Vertebrate Paleontology* 2010;**30**:36–56.

Gardiner BG. The relationships of the palaeoniscid fishes, a review based on new specimens of *Mimia* and *Moythomasia* from the Upper Devonian of Western Australia. *Bulletin of the British Museum (Natural History) Geology* 1984;**37**:175–418.

Giles S, Darras L, Clément G *et al.* An exceptionally preserved Late Devonian actinopterygian provides a new model for primitive cranial anatomy in ray-finned fishes. *Proceedings of the Royal Society B: Biological Sciences* 2015;**282**:20151485. https://doi.org/10.1098/rspb.2015.1485

Heidtke UHJ. Neue Erkenntwisse über *Acanthodes bronni* AGASSIZ 1833. *Mitteilungen der POLLICHIA* 2011;**95**:1–14.

Heidtke UHJ. *Acanthodes bronni*; weitere Exemplare von der Typlokalität Berchweiler bei Kirn. *Mitteilungen der POLLICHIA* 2015;**97**:5–18.
Hodnett JPM, Grogan ED, Lund R *et al*. Ctenacanthiform Sharks from the Late Pennsylvanian (Missourian) Tinijas Member of the Atrasado Formation, Central New Mexico. *New Mexico Museum of Natural History and Science Bulletin* 2021;**84**:391–424.
Hotton N. Jaws and teeth of American xenacanth sharks. *Journal of Paleontology* 1952;**26**:489–500.
Hu Y, Lu J, Young GC. New findings in a 400 million-year-old Devonian placoderm shed light on jaw structure and function in basal gnathostomes. *Scientific Reports* 2017;**7**:1–12.
Jarvik E. The systematic position of acanthodian fishes. In: Andrews SM, Miles RS, Walker A (eds), *Problems in Vertebrate Evolution*. London, UK: Academic Press, 1977, 199–225.
Klug C, Coates M, Frey L *et al*. Broad snouted cladoselachian with sensory specialization at the base of modern chondrichthyans. *Swiss Journal of Palaeontology* 2023;**142**:2.
Long JA, Burrow CJ, Ginter M *et al*. First shark from the Late Devonian (Frasnian) Gogo Formation, Western Australia sheds new light on the development of tessellated calcified cartilage. *PLoS One* 2015;**10**:e0126066. https://doi.org/10.1371/journal.pone.0126066
Maisey JG. An evaluation of jaw suspension in sharks. *American Museum Novitates* 1980;**2706**:1–17.
Maisey JG. Cranial anatomy of the lower Jurassic Shark *Hybodus reticulatus* (Chondrichthyes: Elasmobranchii), with comments on hybodontid systematics. *American Museum Novitates* 1987;**2878**:1–39.
Maisey JG. Visceral skeleton and musculature of a Late Devonian shark. *Journal of Vertebrate Paleontology* 1989;**9**:174–90. https://doi.org/10.1080/02724634.1989.10011751
Maisey JG, Denton JSS, Burrow C *et al*. Architectural and ultrastructural features of tessellated calcified cartilage in modern and extinct chondrichthyan fishes. *Journal of Fish Biology* 2020;**98**:919–41. https://doi.org/10.1111/jfb.14376
Maisey JG, Janvier P, Pradel A *et al*. *Doliodus* and pucapampellids: contrasting perspectives on stem chondrichthyan morphology. In: Johanson Z, Underwood C, Richter M (eds), *Evolution and Development of Fishes*. Cambridge, UK: Cambridge University Press, 2019, 87–109.
Miles RS. A reinterpretation of the visceral skeleton of *Acanthodes*. *Nature* 1964;**204**:457–9. https://doi.org/10.1038/204457a0
Miles RS. Some features in the cranial morphology of acanthodians and the relationships of the Acanthodii. *Acta Zoologica* 1965;**46**:233–55. https://doi.org/10.1111/j.1463-6395.1965.tb00733.x
Miles RS. Jaw articulation and suspension in *Acanthodes* and their significance. In: Ørvig T (ed.), *Current Problems of Lower Vertebrate Phylogeny. Proceedings of the Fourth Nobel Symposium*. Stockholm: Armqvist and Wiksell, 1968, 109–27.
Miles RS. Relationships of acanthodians. In: Greenwood P, Miles RS, Patterson C (eds), *Interrelationships of Fishes*. London, UK: Zoological Journal of the Linnean Society, 1973, 63–103.
Muller M. A quantitative theory of expected volume changes of the mouth during feeding in teleost fishes. *Journal of Zoology* 1989;**217**:639–61. https://doi.org/10.1111/j.1469-7998.1989.tb02515.x
Nelson GJ. Gill-arch structure in Acanthodes. In: Ørvig T (ed.), *Current Problems of Lower Vertebrate Phylogeny. Proc. Fourth Nobel Symp*. Stockholm: Armqvist and Wiksell, 1968, 129–43.
Ørvig T. Histologic studies of placoderms and fossil elasmobranchs. I: The endoskeleton, with remarks on the hard tissues of lower vertebrates in general. *Arkiv för Zoologi* 1951;**2**:321–454.
Ørvig T. Acanthodian dentition and its bearing on the relationships of the group. *Palaeontographica, Abteilung A* 1973;**143**:119–50.
Patterson C. Morphology and interrelationships of primitive actinopterygian fishes. *Integrative and Comparative Biology* 1982;**22**:241–59.
Pradel A, Maisey JG, Tafforeau P *et al*. A Palaeozoic shark with osteichthyan-like branchial arches. *Nature* 2014;**509**:608–11. https://doi.org/10.1038/nature13195
Pradel A, Cuckovic A, Mansuit R *et al*. The visceral skeleton and its relation to the head circulatory system of both a fossil, the Carboniferous *Iniopera*, and a modern, *Callorhinchus* milii holocephalan (Chondrichthyes). In: Pradel A, Denton JSS, Janvier P (eds), *Ancient Fishes and their Living Relatives: A Tribute to John G. Maisey*. Munich: Verlag Dr. Friedrich Pfeil, 2021, 183–92.
Reis OM. Zur Kenntniss des Skeletts der Acanthodinen. *Geognostische Jahreshefte* 1890;**3**:1–66.
Reis OM. Ueber ein Exemplar von *Acanthodes Bronni* Ag. aus der geogn. Sammlung der 'Pollichia'. *Mitt. POLLICHIA* 1894;**8**:316–34.
Reis OM. Illustrationen zur Kenntnis des Skeletts von *Acanthodes bronni* AGASSIZ. *Abhandlungen der Senckenbergischen Naturforschenden Gesellschaft* 1895;**XIX**:49–63.
Reis OM. Ueber *Acanthodes Bronni* Agassiz. *Morphologische Arbeiten* 1896;**6**:143–220.
Schaeffer B. The origin and basic radiation of the Osteichthyes. In: Ørvig T (ed.), *Current Problems of Lower Vertebrate Phylogeny. Proc. Fourth Nobel Symp*. Stockholm: Armqvist and Wiksell, 1968, 207–22.
Schaeffer B, Rosen DE. Major adaptive levels in the evolution of the actinopterygian feeding mechanism. *American Zoologist* 1961;**1**:187–204.
Schultze HP, Zidek J. Ein primitiver acanthodier (pisces) aus dem unterdevon lettlands. *Paläeontologische Zeitschrift* 1982; **56**:95–105.
Stack J, Hodnett JP, Lucas SG *et al*. *Tanyrhinichthys mcallisteri*, a long-rostrumed Pennsylvanian ray-finned fish (Actinopterygii) and the simultaneous appearance of novel ecomorphologies in Late Palaeozoic fishes. *Zoological Journal of the Linnean Society* 2020;**191**:347–74. https://doi.org/10.1093/zoolinnean/zlaa044
Van Wassenbergh S, Leysen H, Adriaens D *et al*. Mechanics of snout expansion in suction-feeding seahorses: musculoskeletal force transmission. *Journal of Experimental Biology* 2013;**216**:407–17. https://doi.org/10.1242/jeb.074658
Véran M. Les éléments accessoires de l'arc hyoidendes poissons téléostomes (Acanthodiens et Osteichthyens) fossiles et actuels. *Mémoires du Muséum national d'histoire naturelle* 1988;**54**:1–98.
Watson DMS. The acanthodian fishes. *Philosophical Transactions of the Royal Society of London, Series B: Biological Sciences* 1937;**228**:49–146.
Zhu M, Yu X, Ahlberg PE *et al*. A Silurian placoderm with osteichthyan-like marginal jaw bones. *Nature* 2013;**502**:188–93. https://doi.org/10.1038/nature12617
Zidek J. Growth in *Acanthodes* (Acanthodii: Pisces) data and implications. *Palaontologische Zeitschrift* 1985;**59**:147–66.